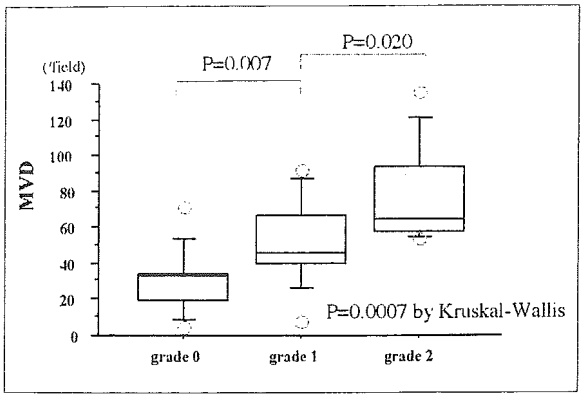

FIGURE 4 MVD in grade 0, grade 1, and grade 2 patients divided according to the count of CD68-positive cells. MVD differed significantly among the three groups ($p=0.0007$, Kruskal-Wallis test). Multiple comparison test showed that MVD differed significantly between grade 0 and grade 1 patients ($p=0.007$), and between grade 1 and grade 2 patients ($p=0.020$). A significant positive correlation was observed between MVD and the ratio of double-immunopositive cells ($p=0.0001$, Spearman rank correlation coefficient = 0.70).

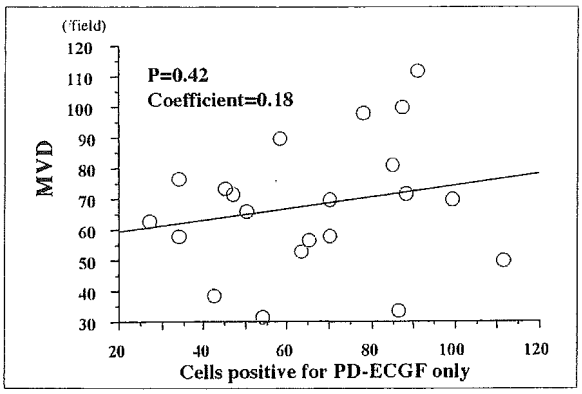

FIGURE 5 Correlation between MVD and cells positive for PD-ECGF alone among non-cancerous cells. No correlation was observed between MVD and the number of cells showing positivity for PD-ECGF alone ($p=0.42$, Spearman rank correlation coefficient=0.18).

MVD and the grade of double immunopositivity ($p=0.0001$, Spearman rank correlation coefficient=0.70). No correlation was observed between MVD and the number of cells showing positivity for PD-ECGF alone ($p=0.42$, Spearman rank correlation coefficient=0.18) **(Figure 5)**.

We also evaluated the relationship between PD-ECGF immunoreactivity in cancer cells and prognosis or MVD. The survival rate of PD-ECGF (+) patients was not significantly different from that of PD-ECGF (-) patients ($p=0.08$). MVD in patients with PD-ECGF (+) and PD-ECGF (-) cancer cells was 48±34.5 and 49.5±24.1, respectively, and the difference was not statistically significant ($p=0.6$).

DISCUSSION

Some previous clinical studies of patients with cholangiocellular carcinoma have shown that lymph node metastasis is associated with a poor prognosis (1-3). Angiogenesis plays an important role in tumor growth and metastasis. Recent studies have shown that MVD in tumors is a major prognostic factor in various forms of cancer including those of the breast, lung, bladder and colon (5,6), although Obermair *et al.* reported that MVD did not seem to be a useful predictor of survival in patients with epithelial ovarian cancer (15). Although there has been no previous report on the relationship between the prognostic significance of MVD in cholangiocellular carcinoma, our present results demonstrate that MVD is an important prognostic factor for patients with this cancer.

Macrophages are the major terminally differentiated cell type of the mononuclear phagocyte system, producing a number of growth stimulators and inhibitors. A number of angiogenic cytokines are known to be produced by macrophages, including VEGF, bFGF, EGF, PD-ECGF, and IL-8. Several studies have demonstrated a relationship between angiogenesis and prognosis in patients with various tumor types (5,16). These studies suggest a close correlation between the number of monocyte/macrophages and angiogenesis in human tumors. In the present study, we found a positive correlation between MVD and the grade of cell double-positivity for CD 68 and PD-ECGF, suggesting that liver macrophages are associated with tumor angiogenesis, and prognostic analysis showed that a higher degree of liver macrophage infiltration was related to poorer prognosis.

Many clinical studies have shown that PD-ECGF is correlated with tumor growth, invasion and metastasis, and some studies have revealed that the expression of PD-ECGF in cancer cells is significantly correlated with intratumoral MVD and metastasis (7-9). Furthermore, a significant correlation between the expression of PD-ECGF in cancer cells and the overall survival of patients has been reported (9,10), whereas it has been shown that PD-ECGF expression in non-cancer cells within the tumor might play an important role in tumor angiogenesis and be a prognostic factor in some malignant tumors (11-13). It has also been reported that PD-ECGF produced by tumor-infiltrating macrophages may play a role in the regulation of cancer cell invasion and distant metastasis (17) and be correlated with increased MVD and poor prognosis (18,19). In the present study, the expression of PD-ECGF in cancer cells was not significantly correlated with angiogenesis or prognosis, and there was no correlation between MVD and the number of non-cancerous cells showing positivity for PD-ECGF alone.

In conclusion, the present findings suggest that liver macrophages at the invasive cancer margin in patients with cholangiocellular carcinoma might participate in tumor angiogenesis through PD-ECGF secretion, and thus influence the prognosis.

REFERENCES

1 **Yamamoto M, Takasaki K, Yoshikawa T:** Lymph node metastasis in intrahepatic cholangiocarcinoma. Jpn J Clin Oncol 1999; 29:147-150.

2 **Inoue K, Makuuchi M, Takayama T, Torzilli G,**

Yamamoto J, Shimada K, Kosuge T, Yamasaki S, Konishi M, Kinoshita T, Miyagawa S, Kawasaki S: *Long-term survival and prognostic factors in the surgical* treatment of mass-forming type cholangiocarcinoma. Surgery 2000; 127:498-505.

3 **Nozaki Y, Yamamoto M, Ikai I, Yamamoto Y, Ozaki N, Fujii H, Nagahori K, Matsumoto Y, Yamaoka Y:** *Reconsideration of the lymph node metastasis pattern* (N factor) from intrahepatic cholangiocarcinoma using the International Union Against Cancer TNM staging system for primary liver carcinoma. Cancer 1998; 83:1923-1929.

4 **Weidner N, Semple JP, Welch WR, Folkman J:** Tumor angiogenesis and metastasis - correlation in invasive breast carcinoma. N Engl J Med 1991; 324:1-8.

5 **Leek RD, Lewis CE, Whitehouse R, Greenall M, Clarke J, Harris AL:** Association of macrophage infiltration with angiogenesis and prognosis in invasive breast carcinoma. Cancer Res 1996; 56:4625-4629.

6 **Orre M, Rogers PA:** Macrophages and microvessel density in tumors of the ovary. Gynecol Oncol 1999; 73:47-50.

7 **Toi M, Hoshina S, Taniguchi T, Yamamoto Y, Ishitsuka H, Tominaga T:** Expression of platelet-derived endothelial cell growth factor/thymidine phosphorylase in human breast cancer. Int J Cancer 1995; 64:79-82.

8 **Koukourakis MI, Giatromanolaki A, O'Byrne KJ, Comley M, Whitehouse RM, Talbot DC, Gatter KC, Harris AL:** Platelet-derived endothelial cell growth factor expression correlates with tumour angiogenesis and prognosis in non-small-cell lung cancer. Br J Cancer 1997; 75:477-481.

9 **Takebayashi Y, Akiyama S, Akiba S, Yamada K, Miyadera K, Sumizawa T, Yamada Y, Murata F, Aikou T:** Clinicopathologic and prognostic significance of an angiogenic factor, thymidine phosphorylase, in human colorectal carcinoma. J Natl Cancer Inst 1996; 88:1110-1117.

10 **Maeda K, Chung YS, Ogawa Y, Takatsuka S, Kang SM, Ogawa M, Sawada T, Onoda N, Kato Y, Sowa M:** Thymidine phosphorylase/platelet-derived endothelial cell growth factor expression associated with hepatic metastasis in gastric carcinoma. Br J Cancer 1996; 73:884-888.

11 **Okada K, Yokoyama K, Okihara K, Ukimura O, Kojima M, Miki T, Takamatsu T:** Immunohistochemical localization of platelet-derived endothelial cell growth factor expression and its relation to angiogenesis in prostate. Urology 2001; 57:376-381.

12 **Fujioka S, Yoshida K, Yanagisawa S, Kawakami M, Aoki T, Yamazaki Y:** Angiogenesis in pancreatic carcinoma: thymidine phosphorylase expression in stromal cells and intratumoral microvessel density as independent predictors of overall and relapse-free survival. Cancer 2001; 92:1788-1797.

13 **Kojima H, Shijubo N, Abe S:** Thymidine phosphorylase and vascular endothelial growth factor in patients with Stage I lung adenocarcinoma. Cancer 2002; 94:1083-1093.

14 **Matsumura M, Chiba Y, Lu C, Amaya H, Shimomatsuya T, Horiuchi T, Muraoka R, Tanigawa N:** Platelet-derived endothelial cell growth factor/thymidine phosphorylase expression correlated with tumor angiogenesis and macrophage infiltration in colorectal cancer. Cancer Lett 1998; 128:55-63.

15 **Obermair A, Wasicky R, Kaider A, Preyer O, Losch A, Leodolter S, Kolbl H:** Prognostic significance of tumor angiogenesis in epithelial ovarian cancer. Cancer Lett 1999; 138:175-182.

16 **Salvesen HB, Akslen LA:** Significance of tumour-associated macrophages, vascular endothelial growth factor and thrombospondin-1 expression for tumour angiogenesis and prognosis in endometrial carcinomas. Int J Cancer 1999; 84:538-543.

17 **Tanaka Y, Kobayashi H, Suzuki M, Kanayama N, Suzuki M, Terao T:** Thymidine phosphorylase expression in tumor-infiltrating macrophages may be correlated with poor prognosis in uterine endometrial cancer. Hum Pathol 2002; 33:1105-1113.

18 **Yao Y, Kubota T, Sato K, Kitai R:** Macrophage infiltration-associated thymidine phosphorylase expression correlates with increased microvessel density and poor prognosis in astrocytic tumors. Clin Cancer Res 2001; 7:4021-4026.

19 **Parker C, Milosevic M, Panzarella T, Banerjee D, Jewett M, Catton C, Tew-George B, Gospodarowicz M, Warde P:** The prognostic significance of the tumour infiltrating lymphocyte count in stage I testicular seminoma managed by surveillance. Eur J Cancer 2002; 38:2014-2019.

STEM CELLS®
Original Article

Crucial Roles of Mesodermal Cell Lineages in a Murine Embryonic Stem Cell–Derived In Vitro Liver Organogenesis System

SHINICHIRO OGAWA,[a,b] YOH-ICHI TAGAWA,[a] AKIKO KAMIYOSHI,[a] AKIHIRO SUZUKI,[a] JUN NAKAYAMA,[c] YASUHIKO HASHIKURA,[b] SHINICHI MIYAGAWA[b]

[a]Division of Laboratory Animal Research, Research Center for Human and Environmental Sciences, Shinshu University;
[b]Department of Surgery, Shinshu University School of Medicine;
[c]Department of Pathology, Shinshu University School of Medicine, Shinshu, Japan

Key Words. Embryonic stem cell • Liver • Organogenesis • Cardiomyocyte • Endothelial cell • In vitro system

ABSTRACT

Recent studies in the field of regenerative medicine have exploited the pluripotency of embryonic stem (ES) cells to generate a variety of cell lineages. However, the target has always been only a single lineage, which was isolated from other differentiated cell populations. In the present study, we selected sublines with a high capability for differentiation to contracting cardiomyocytes and also produced germline chimeric mice from a parent ES line. We also succeed in establishing embryoid bodies prepared from the ES cells that differentiated into not only hepatocytes but also at least two mesodermal lineages: cardiomyocytes that supported liver development and endothelial cells corresponding to sinusoids. This allowed the development of an in vitro system using murine ES cells that approximated the events of liver development in vivo. The expression of *albumin* was significantly higher in cardiomyocytes that had arisen in differentiated ES cells than in those that had not. Our in vitro system for liver organogenesis consists of a blood/sinusoid vascular-like network and hepatocyte layers and shows higher levels of hepatic function, such as albumin production and ammonia degradation, than hepatic cell lines and primary cultures of murine adult hepatocytes. This innovative system will lead to the development of second-generation regenerative medicine techniques using ES cells and is expected to be useful for the development of bioartificial liver systems and drug-metabolism assays. STEM CELLS *2005;23:903–913*

INTRODUCTION

The liver develops from the ventral foregut in vertebrates, receiving multiple stimuli in the form of growth factors, cytokines, and hormonal factors, as well as intercellular and matrix cellular interactions [1–5]. In particular, the precardiac mesoderm produces factors that trigger hepatic development [6, 7], that is, cardiomyocytes support liver organogenesis (Fig. 7A). The signaling of fibroblast growth factor (FGF), produced in the cardiac mesoderm, induces the initial step of hepatogenesis in the ventral endoderm at E8.5–9.5 of mouse development, resulting in the activation of albumin and α-fetoprotein expressions [4, 6, 8]. As the hepatic precursor cells migrate into the septum transversum to form a liver bud [9], endothelial progenitor cells arise there simultaneously in close association with early developing hepatoblasts and hepatogenesis [10]. These endothelial cells develop a fenestrated morphology to form the hepatic sinusoids [11–13], and then finally the liver is completed, with its multiple and specific functions.

In the field of regenerative medicine, the pluripotency of embryonic stem (ES) cells has been applied to obtain a vari-

Correspondence: Yoh-ichi Tagawa, Ph.D., Department of Biomolecular Engineering, Graduate School of Bioscience and Biotechnology, Tokyo Institute of Technology, B-51 4259 Nagatsuta-cho, Midori-ku, Yokohama, Kanagawa, 226-8501 Japan. Telephone: 81-45-924-5791; Fax: 81-45-924-5815; e-mail: ytagawa@bio.titech.ac.jp Received October 23, 2004; accepted for publication March 20, 2005.
 1066-5099/2005/$12.00/0 doi: 10.1634/stemcells.2004-0295

ety of cell lineages. However, the targets of these systems have always been limited to only a single lineage, which was isolated from other differentiated cell populations. There have been a few reports on the differentiation of murine ES cells to hepatocyte-like or albumin-producing cells [14–19]. However, these studies focused only on hepatocytes as a single-cell lineage and did not refer to liver organogenesis. It also has been reported that hepatocyte-like cells spontaneously differentiate from human ES cells [20], as well as previous studies using murine ES cells. In particular, there has been no description about the roles of cardiomyocytes and endothelial cells in hepatocyte differentiation, although one previous study has detected albumin-positive cells adjacent to cardiomyocytes in teratoma-derived human ES cells in severe combined immunodeficiency mice [20]. Cardiac mesoderm has a strong capacity to induce liver organogenesis [4, 6, 8]. These cell lineages can also be obtained from ES cells. Therefore, we considered that emergence of cardiomyocytes would be necessary for liver morphogenesis from ES cells in vitro. Our purpose in the present study was to establish a system for in vitro hepatic morphogenesis consisting of not only hepatocytes but also cell lineages supporting hepatic differentiation, such as cardiomyocytes and endothelial cells, which correspond to those involved in liver organogenesis in vivo, from murine ES cells. We exploited the pluripotency of ES cells for differentiation of these cell lineages, which included hepatocytes, cardiomyocytes, and endothelial cells, and succeeded in establishing a novel system of hepatic morphogenesis from murine ES cells based on naturally occurring embryological events, that is, with contributions from cardiac mesoderm and endothelial cell lineages.

Materials and Methods

Cell Culture

E14-1 ES cells derived from 129/Ola were grown on mitomycin C–treated mouse embryonic fibroblast feeder layers to maintain them in an undifferentiated state in Dulbecco's modified Eagle's medium (DMEM) (Invitrogen, Tokyo, http://www.invitrogen.com) containing 20% fetal bovine serum (FBS) (Hyclone, Logan, UT, http://www.hyclone.com), 1 mM sodium pyruvate (Invitrogen), 100 μM nonessential amino acids (Invitrogen), 100 μM 2-mercaptoethanol (Sigma, St. Louis, http://www.sigmaaldrich.com), and 10^3 U/ml leukemia inhibitory factor (LIF) (Chemicon, CA, http://www.chemicon.com). The cells were dissociated with 0.25% trypsin, 1% chicken serum (Invitrogen), and 1 mM EDTA in phosphate-buffered saline (PBS) and resuspended in Iscove's modified Dulbecco's medium (IMDM) (Invitrogen) containing 20% FBS, 1 mM sodium pyruvate, 100 μM nonessential amino acids, and 100 μM 2-mercaptoethanol without LIF and then formed into a hanging drop at a concentration of 1,000 cells per 50-μl drop. The hanging drop was cultured in an atmosphere of 5% CO_2 at 37°C for 5 days. An individual 5-day-old embryoid body (EB) was plated in each well of a gelatin-coated 96-well plate, and the growth factor was added to the culture medium. The day when the 5-day-old EBs were plated in the dish was denoted day 0 (A0). Human recombinant acidic fibroblast growth factor (aFGF) (Invitrogen) was added to the differentiation medium at a concentration of 100 ng/ml 2 days after plating of the 5-day-old EBs (A2), and 20 ng/ml human recombinant hepatocyte growth factor (HGF) (Genzyme/Techne, Minneapolis, http://www.g-tonline.com) was added at A4. Then, at A6, 10 ng/ml mouse recombinant oncostatin M (Genzyme/Techne), 100 nM dexamethasone (MP Biomedicals, Irvine, CA, http://www.mpbio.com), ITS (insulin 10 μg/ml, transferrin 5 μg/ml, selenium 5 ng/ml; Invitrogen), and 10 mM nicotinamide (Nakalai tesque, Kyoto, Japan, http://www.nacalai.co.jp) were added. The emergence frequency of contracting cells in the EB outgrowths, indicating cardiac muscle differentiation, was monitored daily. Emergence frequency was expressed as a percentage, where 100% meant detection of a contractile area in all wells containing EB outgrowths. Twenty recloned 5-day-old EBs were plated on a 6-cm dish coated with gelatin as a semi–large-scale culture.

To obtain fetal hepatocytes, mouse liver at E15 was minced and dissociated with collagenase II (Sigma) in Hanks' buffer (Invitrogen). The cells were seeded on a gelatin-coated dish in DMEM supplemented with 10% FBS, 100 μM nonessential amino acids, and 100 U/ml penicillin-100 μg/ml streptomycin-292 μg/ml glutamine for a few hours and washed once with the same medium. The medium was replaced every day.

Primary adult hepatocytes were isolated from male 129/SvJ mice by the two-step collagenase perfusion method. The hepatocytes were separated from the resulting cell suspension by centrifugation and then by centrifugation through a 50% Percoll (Sigma) gradient. Isolated hepatocytes were plated onto gelatin-coated dishes.

Production of Chimeric Mice

Chimeric mice were produced by the modified aggregation method [21]. This involved aggregation of 10 to 15 ES cells with two (BDF1 × C57BL) F_1 eight-cell-stage embryos, from which the zona pellucida had been removed with Tyrode's solution (Sigma), were placed in a hole on a plastic dish and cultured overnight. The ES cells and eight-cell-stage embryos became a single blastocyst, and the blastocysts were then transferred to the uterus of pseudopregnant female ICR mice. Male chimeric mice were then bred with C57BL/6 female mice, and germ-line transmission of the ES cells was checked by the agouti coat color of the offspring.

RNA Extraction and Reverse Transcription–Polymerase Chain Reaction Analysis

Total RNA was extracted from the outgrowths of the EBs using a MagEXtractor mRNA kit (Toyobo, Tokyo, http://www.toyobo.co.jp/e). Briefly, 2-μg aliquots of total RNA were reverse tran-

scribed to cDNAs using a Superscript II first-strand synthesis system with an oligo dT primer (Invitrogen). Semiquantitative reverse transcription–polymerase chain reaction (RT-PCR) was performed using Ex Taq DNA polymerase (Takara, Tokyo, http://www.takara-bio.com) with the following primer sets. For each experiment, a housekeeping gene, hypoxanthine phosphoribosyltransferase, was amplified with 25 cycles to normalize the expressions of other genes in the sample. The forward and reverse primers were located at different exons to discriminate the product from the targeted mRNA or its genomic DNA. The PCR primers used were as follows: albumin, GCTACGGCACAGTGCTTG and CAGGATTGCAGACAGATAGTC (product size, 265 bp; annealing temperature, 65°C); α-fetoprotein, TCGTATTCCAACAGGAGG and AGGCTTTTGCTTCACCAG (product size, 173 bp; annealing temperature, 65°C); transthyretin, CTCACCACAGATGAGAAG and GGCTGAGTCTCTCAATTC (product size, 223 bp; annealing temperature, 56°C); α1–anti-trypsin, AATGGAAGAAGCCATTCGAT and AAGACTGTAGCTGCTGCAGC (product size, 483 bp; annealing temperature, 50°C); Oct3/4, AGCACGAGTGGAAAGCACT and CTCATTGTTGTCGGCTTCCT (product size, 339 bp; annealing temperature, 60°C); tyrosine aminotransferase, ACCTTCAATCCCATCCGA and TCCCGACTGGATAGGTAG (product size, 205 bp; annealing temperature, 66°C); tryptophan 2,3-deoxygenase, TGCGCAAGAACTTCAGAGTGA and TGCGCAAGAACTTCAGAGTGA (product size, 419 bp; annealing temperature, 62°C); liver-specific organic anion transporter-1, TGCGCAAGAACTTCAGAGTGA and TGAGTTGGACCCCTTTTCAC (product size, 226 bp; annealing temperature, 65°C); asialoglycoprotein receptor-1, GCTGGAAAAACAGCAGAAGG and CTGTTCCATCCACCCATTTC (product size, 358 bp; annealing temperature, 65°C); asialoglycoprotein receptor-2, CGGACCCTGAAAGAAACCTT and ATGAAACTGGCTCCTGTGCT (product size, 410 bp; annealing temperature, 66°C); HGF, AGACACCACACCGGCACAGT and ATAGGGCAATAATCCCAAGG (product size, 484 bp; annealing temperature, 65°C); FGF-1, ACCGAGAGGTTCAACCTGCC and GCCATAGTGAGTCCGAGGACC (product size, 386 bp; annealing temperature, 66°C); vascular endothelial growth factor (VEGF), CAGGCTGCTGTAACGATGAA and AATGCTTTCTCCGCTCTGAA (product size, 206 bp; annealing temperature, 65°C); VEGFR1, TGTGGAGAAACTTGGTGACCT and TGGAGAACAGCAGGACTCCTT (product size, 504 bp; annealing temperature, 65°C); VEGFR2, TCTGTGGTTCTGCGTGGAGA and GTATCATTTCCAACCACCC (product size, 269 bp; annealing temperature, 55°C); platelet-endothelial cell adhesion molecule-1 (PECAM-1), GTCATGGCCATGGTCGAGTA and AGCAGGACAGGTCCAACAAC (product size, 168 bp; annealing temperature, 65°C); atrial natriuretic peptide, ATGGGCTCCTTCTCCCATCAC and TGTTGCAGCCTAGTCCACTC (product size, 541 bp; annealing temperature, 65°C); and hypoxanthine phosphoribosyltransferase, GTTGGATACAGGCCAGACTTTGTTG and GAGGGTAGGCTGGCCTATAGGCT (product size, 269 bp; annealing temperature, 65°C).

Immunohistochemical Analysis

Twenty EBs were cultured on gelatin-coated glass coverslips in a six-well plate. EB outgrowths on the coverslips were fixed with 4% paraformaldehyde/PBS for 20 minutes and then permeabilized with 0.1% Triton X for 10 minutes at room temperature. The fixed samples were incubated in blocking buffer containing 4% donkey serum (Jackson Immunoresearch, Baltimore, http://www.jacksonimmuno.com) for 10 minutes at room temperature. They were then incubated with the primary antibody overnight at 4°C and with the secondary antibody for 1 hour in a humidified chamber. The following antibodies were used: rabbit immunoglobulin (IgG) against mouse albumin (1:250; MP Biomedicals), goat IgG against mouse PECAM-1 (1:250; Santa Cruz Biotech, CA, http://www.scbt.com), tetramethylrhodamine isothiocyanate–conjugated swine anti-rabbit immunoglobulin (1:60; DakoCytomation A/S, Glostrup, Denmark, http://www.dakocytomation.com), and fluorescein-conjugated donkey anti-goat IgG (1:100; Jackson Immunoresearch, West Grove, PA). For nuclear staining, the cells were incubated for 5 minutes at room temperature with DAPI (4,6 diamidino-2-phenylindole). The samples were mounted in DakoCytomation fluorescent mounting medium and observed using a fluorescence microscope (BX 60; Olympus, Tokyo, http://www.olympus-global.com/en/global) and a confocal laser microscope (TCS SP2; Leica, Manheim, Germany, http://www.leica.com/index.html).

Western Blotting Analysis

ES cells and EBs were homogenized in buffer containing 20 mM Tris-HCl, pH 7.5, 150 mM NaCl, 1% Nonidet P-40, 0.1% SDS, 1% sodium deoxycholate, 2 mM EDTA, 1 mM phenylmethylsulfonyl fluoride, 2 μg/ml aprotinin, 10 μg/ml leupeptin, and 5 μg/ml pepstatin, centrifuged at 12,000 rpm for 10 minutes at 4°C, and the supernatants were collected. Protein concentration was measured with a bicinchoninic acid protein assay (BCA protein assay kit; Pierce, Rockford, IL, http://www.piercenet.com). The same amounts (10 μg each lane) of proteins from cell homogenates were electrophoresed on 8% polyacrylamide gels. Proteins were transferred onto polyvinylidene difluoride membranes by electro blotting. The membranes were blocked for 1 hour at room temperature with 5% nonfat dried milk and 0.1% bovine serum albumin in tris-buffered saline (TBS) containing 0.1% (vol/vol) Tween 20 (TBS-T) and incubated for 1 hour with peroxidase-conjugated sheep anti-rabbit antibody (GE Healthcare, Piscataway, NJ, http://www.gehealthcare.com) diluted in TBS-T containing 5% FBS. After washing with TBS-T, the blots

were developed by enhanced chemiluminescence (GE Healthcare) and exposed to x-ray film (RX-U; Fuji, Kawasaki, Japan, http://home.fujifilm.com).

Treatment with Thalidomide or CBO-P11

Thalidomide (N-[2,6-dioxo-3-piperidinyl] phthalimide; Tocris Cookson, Ellisville, MO, http://www.tocris.com) was dissolved in dimethyl sulfoxide and added to the medium at the indicated concentration. CBO-P11 (cyclo-VEGI) (DFPQIMRIKPHQGQHIGE) (Calbiochem, San Diego, http://www.emdbiosciences.com/html/CBC/home.html), a cyclopeptidic vascular endothelial growth inhibitor, was dissolved in water and added to the medium at a concentration of 10 μM. These chemicals were added to the medium after 20 five-day-old EBs had been plated on the dish (A0). The medium was replaced every day.

Ammonia Modification Function Assay

To examine cellular ammonia degradation activity, 2 mM NH_4Cl was added to the serum-free culture medium of 30 or 50 EBs at days 10 and 18 after plating and further incubated for 24 hours. The concentration of NH_4Cl remaining in the medium was measured at various time points by a modified indophenol method using a commercial kit (Ammonia-test Wako; Wako, Osaka, Japan, http://www.wako-chem.co.jp).

Results

Roles of Embryonic Stem Cell–Derived Cardiomyocytes in Hepatic Differentiation from Murine Embryonic Stem Cells

As is the case in in vivo development, the emergence of cardiomyocytes is necessary for liver organogenesis in an in vitro differentiation system using ES cells. As an initial approach for inducing murine ES cells to undergo hepatic morphogenesis, we established a system for spontaneous differentiation to contracting cardiomyocytes with a high frequency of emergence. A single 5-day-old EB comprised of dissociated murine ES cells was plated onto gelatin-coated plates and allowed to adhere to the bottom of the plate. The EB outgrowths began to contract spontaneously within 5 days after plating. These ES cell–derived contracting cells were considered to be cardiomyocytes based on specific gene expression (Fig. 1B) and pharmacological responses. The outgrowths of EBs were cultured in the differentiation medium for 18 days (A18) after adhesion to the well bottom. The expression of *albumin* was compared in groups of EBs in which cardiomyocytes had and had not arisen at A10; the levels of albumin expression were significantly higher in those with outgrowths of contracting cardiomyocytes than in those without (Fig. 1B), suggesting that the ability to differentiate to cardiomyocytes in the ES cell population and the emergence of cardiomyocytes in the EB outgrowths are important for endodermal and hepatocyte differentiation.

To increase the efficiency of liver organogenesis from ES cells, it was considered important to increase the frequency of cardiomyocyte emergence in the EB outgrowths. The frequency of cardiomyocyte emergence at Ab-3 was less than 30% using the parental line of the E14-1 ES cells at passages 14 through 18, whereas the frequency was almost 100% using some sublines (My-1 and Ab-3) other than My-5, which were recloned from the parental line E14-1 (Fig. 1A). Ability for the production of chimeric mice was also compared in the parental line and these E14-1 sublines. The chimera-forming ability of the parental E14-1 was 2 germ-line/17 chimeric mice from

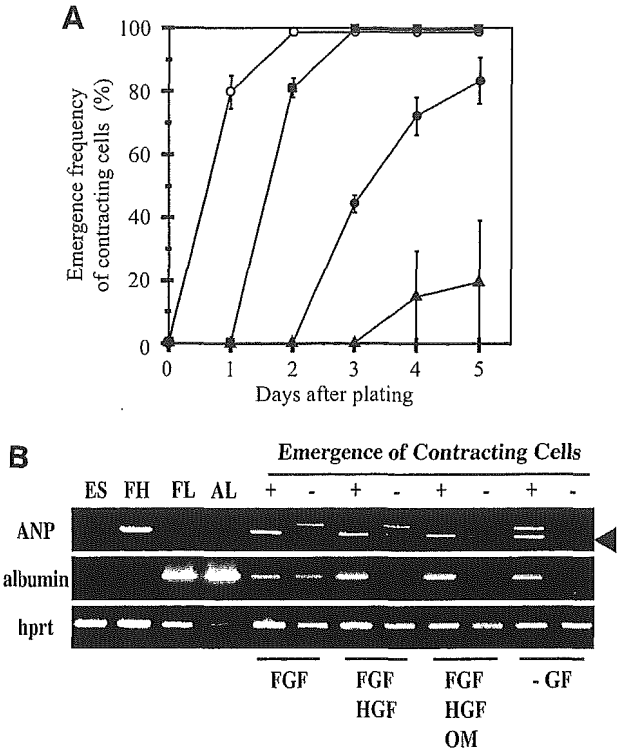

Figure 1. Establishment of a system for allowing differentiation of ES cells to cardiomyocytes at a frequency of almost 100% for hepatic differentiation. **(A):** Comparison of the time courses of the frequency of emergence contractile cells from outgrowths of EBs prepared from the parental line of E14-1 ES cells (●), subline My-1 (○), Ab-3 (■), and My-5 (▲). **(B):** Expression of albumin as a representative hepatic marker and of ANP as an atrial marker was determined by reverse transcription–PCR during differentiation of EBs. PCR amplication of ANP and albumin was carried out for 30 cycles. Human recombinant aFGF was added to the differentiation medium at a concentration of 100 ng/ml 2 days after plating of the 5-day-old EBs on the dish (A2), and then 20 ng/ml human recombinant HGF was added at A4. Then with 10 ng/ml mouse recombinant OSM, 100 nM dexamethasone, ITS (insulin 10 μg/ml, transferrin 5 μg/ ml, selenium 5 ng/ml), and 10 mM nicotinamide (Nacalai) were added at A6. Arrowhead indicates the expected band of ANP. Abbreviations: aFGF, acidic fibroblast growth factor; AL, mouse adult liver; ANP, atrial natriuretic peptide; EB, embryoid body; ES, embryonic stem; GF, growth factor; FH, mouse fetal heart at E15; FL, mouse fetal liver at E15; HGF, hepatocyte growth factor; OSM, oncostatin M; PCR, polymerase chain reaction.

171 ES-aggregated embryos, whereas that of a subline Ab-3 was 4 germ-line/18 chimeric mice from 155 ES-aggregated embryos. It is very important that undifferentiated and pluripotent ES cells should be present in these cultures for differentiation not only to cardiomyocytes but also to albumin-producing hepatocytes and endothelial cells corresponding to the developmental stages of the liver. For the following experiments, we used the selected subline, Ab-3, which showed high capability for differentiation to cardiomyocytes and also for production of germ-line chimeric mice, within six passages.

Expression and Function of Liver-Specific Gene Expressions and Functions in Murine Embryonic Stem Cell–Derived Hepatic Morphogenesis

Twenty 5-day-old EBs were placed together on gelatin-coated dishes in differentiation medium as a semi–large-scale system, because the absolute numbers of cells would be needed for hepatic development. Contracting cardiomyocytes emerged in the central area of EB outgrowth. A heterologous population was considered important for in vitro hepatic morphogenesis using murine ES cells. The expressions of endodermal/hepatocyte-specific genes, such as transthyretin, α-fetoprotein, α1-antitrypsin, and albumin, at the various stages of EB differentiation were examined (Fig. 2A). The levels of expression of these genes increased markedly as differentiation of the EBs proceeded, whereas that of *Oct-3/4*, a marker of undifferentiated ES cells, decreased. The levels of expression of liver-specific genes and *Oct-3/4* in the presence of growth factor were the same as those in the absence of growth factor, suggesting that cardiomyocytes were not induced in the presence of growth factor. We also confirmed that albumin protein was detectable in the differentiated outgrowths of EBs at A4 and increased gradually throughout differentiation (Fig. 2B), corresponding to the changes in mRNA levels (Fig. 2A).

As a second approach for inducing hepatic morphogenesis from ES cells, aFGF, HGF, and oncostatin M were added to the cultures to investigate the effects of growth factors. The levels of expression of albumin, tyrosine aminotransferase (*TAT*), and tryptophan oxygenase (*TO*) were significantly higher in the presence than in the absence of additional growth factors at A10, corresponding to the early differentiation stage of EBs. This suggests that the addition of growth factors artificially induces the expression of mature hepatocyte-specific genes or accelerates differentiation in the system at an early stage (Fig. 2C). On the other hand, at A18, corresponding to the late differentiation stage, the levels of expression of albumin, *TAT*, *TO*, and asialo glycoprotein receptors (*ASGR1, ASGR2*) in the EB were almost the same levels under conditions with and without

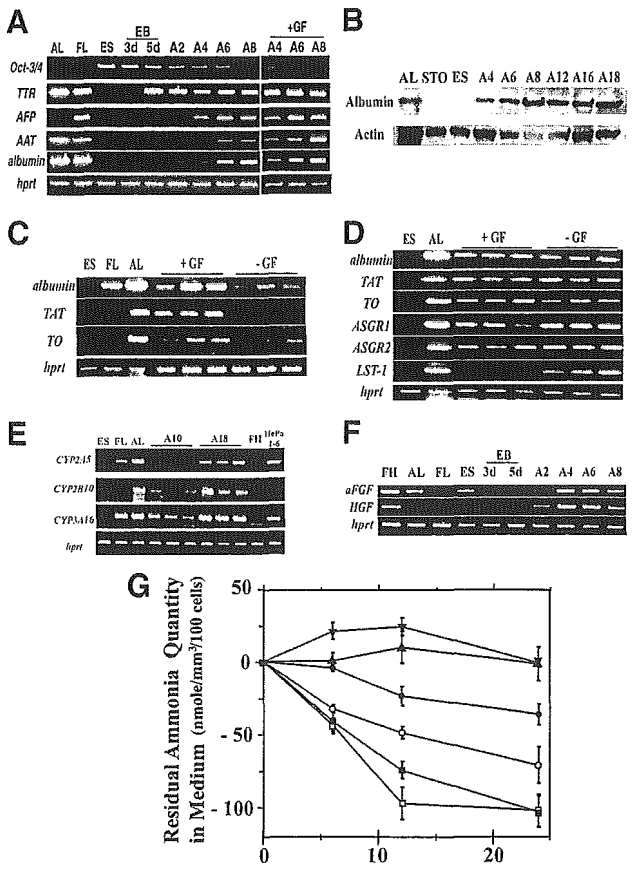

Figure 2. Expression by ES cell–derived hepatocytes of a variety of liver-specific genes, production of albumin protein, and ammonia modification function. **(A):** The expression of endodermal-specific genes was examined in the outgrowths of EBs from before plating (3- and 5-day-old EBs) to 8 days after plating (A8) by RT-PCR. PCR amplification of *Oct-3/4, TTR, AFP, AAT,* and *albumin* was carried out for 30 cycles. Five-day-old EBs were plated on gelatin-coated dishes and cultured in the absence of any growth factors. **(B):** The level of albumin protein was quantified by Western blotting analysis during hepatic differentiation of EBs. EBs were cultured in the absence of any growth factors for 18 days. **(C, D):** Expression of albumin and mature hepatocyte-specific genes expression was detected in the EB outgrowths at A10 **(C)** and A18 **(D)**. Comparison of cultures in the presence or absence of additional growth factors. PCR amplification of *albumin* was carried out for 25 cycles. Amplification of TAT, ASGR-1, ASGR-2, and LST-1 was carried out for 40 cycles. Amplification of TO was carried out for 30 cycles. **(E):** Expression of CYP family genes, such as Cyp2A5, 2B10, and 3A16, was detected by RT-PCR (40 cycles, respectively) in the EB outgrowths at A10 and A18 cultured in the absence of additional growth factors. **(G):** Ammonia modification function was measured in EB outgrowths at A18. The amounts of residual ammonia in 100 cells are indicated, which were calculated from the quantity of prepared genomic DNA. □, primary adult mouse hepatocyte culture; ■, outgrowth of 50 EBs at A18; ○, 30 EBs at A18; ●, 30 EBs at A10; ▼, mouse hepatoma cell line, HePa1–6; ▲, ES E14-1. **(F):** Endogenous aFGF and HGF gene expression was detected by RT-PCR (40 cycles, respectively) in the EB outgrowths during differentiation in the absence of these additional growth factors by RT-PCR. Arrowhead indicates the expected band of ANP. Abbreviations: aFGF, acidic fibroblast growth factor; AL, mouse adult liver; EB, embryoid body; ES, embryonic stem; GF, growth factor; FL, mouse fetal liver at E15; HGF, hepatocyte growth factor; RT-PCR, reverse transcription–polymerase chain reaction ; TAT, tyrosine aminotransferase.

additional growth factors. Furthermore, *liver-specific transporter (LST-1)* mRNA was detected only in the absence of any growth factor (Fig. 2D), suggesting that these additional factors were not essential for hepatic differentiation and maturation from ES cells in our system. The expressions of some CYP genes were also detectable under conditions without growth factors (Fig. 2E).

To investigate whether the outgrowths of EBs could supply these growth factors themselves, the expressions of these genes were analyzed in EBs without these growth factors. Endogenous *aFGF* and *HGF* expression was detected in the outgrowths in the absence of the additional growth factors (Fig. 2F), suggesting that addition of these growth factors is not necessary for hepatic differentiation of EBs, as they are produced endogenously.

Assay of ammonia degradation, a representative hepatic function, was also carried out. Interestingly, the level of ammonia degradation was markedly higher in the differentiated EB outgrowths than in the hepatocyte cell line, HePa1-6, and in primary cultures of murine hepatocytes (Fig. 2E).

To investigate the distribution of albumin-positive cells in the EB outgrowths at A10 and A18, we performed immunohistochemical analyses using anti-mouse albumin antibody. The albumin-positive cells were visualized adjacent to the contracting cardiomyocytes, around the central area of the outgrowths, at A10 (Fig. 3A). These albumin-positive cells formed clusters and showed an islet-like morphology in the outgrowths (Figs. 3A, 3B). At A18, corresponding to the late stage of hepatic differentiation, these colonies had grown and were strongly detected, as can be seen in Figure 3C, suggesting that these cells were proliferating and expanding.

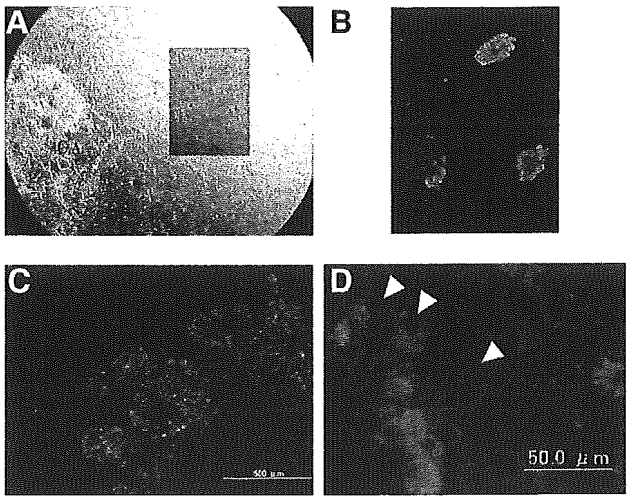

Figure 3. Albumin-positive cells observed as expanding colonies in the outgrowths of EBs. **(A):** Photomicrograph showing the contracting region and albumin-positive areas in the outgrowths of differentiated EBs at A10 in the absence of any growth factors. The shaded square is magnified in **(B)**. **(B–D):** Immunohistochemical analysis of the EB outgrowths at **(B)** A10 and **(C, D)** A18 using anti-albumin (red). White arrowheads indicate the binuclear cells in the outgrowths of the EB. These cultures were also carried out in the absence of any growth factors. Abbreviations: CA, contracting cardiomyocyte area; EB, embryoid body.

Morphology of Murine Embryonic Stem Cell–Derived Hepatocytes

Murine hepatocytes contained two morphologically distinct populations, a mononuclear population and a binuclear population. Hepatocytes in the resting liver consist predominantly of binuclear hepatocytes, whereas those in the regenerating liver are mainly mononuclear hepatocytes [22]. Some of these albumin-positive cells were binuclear, which is a characteristic of mature hepatocytes in mice (Fig. 3D). Thus, these cells were confirmed to be murine hepatocytes on the basis of morphology as well as by hepatic function and gene expression analysis. In addition to hepatic function and expression in our cultures, morphological evidence also suggested that the albumin-producing cells derived from ES cells in our system were hepatocytes.

Vasculogenesis in the System to Induce Murine Embryonic Stem Cells to Hepatic Morphogenesis

The contribution of the nonparenchymal hepatic cell population is necessary for hepatic in vitro morphogenesis from ES cells. Expression of *VEGF, VEGFR1,* and *VEGFR2* was detected from the EB in the period from before plating to the late stage of differentiated EB, and *CD31/PECAM-1,* a definitive endothelial cell–specific marker, began to be expressed at the stage of EB formation and continued to be detectable until the late stage of differentiation of the EB outgrowths (Fig. 4A), suggesting that vasculogenesis had been activated in this system. Indeed, CD31/PECAM-1–positive cells were shown to form network structures (Fig. 4C), indicating that CD31/PECAM-1–positive cells organized the formation of vascular networks in the EB outgrowths. In the presence of additional growth factors, few CD31/PECAM-1–positive cells were seen to be organizing capillary networks, which were twisted and slender (Fig. 4D), compared with those in the absence of additional growth factors.

To analyze the interactions between albumin-producing cells and these endothelial cells, the EB outgrowths at both the early and late stages after plating were stained with anti-albumin and anti-CD31/PECAM-1 antibodies. Using these antibodies discriminated parenchymal or nonparenchymal cells as anti-albumin–positive or anti-CD31/PECAM-1–positive cells, respectively, in mixed control cultures of cells prepared from mouse liver (Fig. 4B). Interestingly, the CD31/PECAM-1–positive cells were seen to be migrating in the albumin-positive areas of the EB outgrowths at A10 and made contact with the juxtapositions of the albumin-positive cells (Fig. 4E), similar to the situation liver organogenesis in the developing embryo [10]. As can be seen in Figures 4E and 4F, albumin-positive cells were proliferating from A10 to A18. The CD31/PECAM-1–positive cells were seen to be

proliferating and organizing networks with the spread of the albumin-positive area in the EB outgrowths at A18 (Fig. 4F), suggesting that these endothelial cells had a marked influence on formation of hepatic tissue within EBs.

To obtain conclusive evidence that vasculogenesis was necessary for hepatocytes to arise and grow in the EB outgrowth, vasculogenesis was inhibited by addition of thalidomide to the differentiation medium. First, the emergence frequency of contracting cardiomyocytes was significantly lower with the addition of thalidomide (26.7% ± 12.0% at 25 mg/L, 6.8% ± 4.2% at 100 mg/L) at A3 than without thalidomide (99.5% ± 0.5%), suggesting that thalidomide was able to inhibit the differentiation of ES cells to cardiomyocytes. The results of confocal microscopy analysis (Figs. 5A–5C) indicated that thalidomide could strongly inhibit the differentiation of CD31/PECAM-1–positive cells in the EB outgrowths compared with the control cultures without thalidomide. In addition, the albumin-positive area was significantly smaller in differentiated EB outgrowths exposed to thalidomide at A18 compared with the control culture in the absence of thalidomide (Fig. 5A), and the density and area of the vascular-like network consisting of ES-derived CD31/PECAM-1–positive endothelial cells were much lower in the thalidomide-treated EB outgrowths than in the absence of thalidomide. The expression of *VEGFR1, VEGFR2*, and *PECAM-1* was inhibited by thalidomide in a dose-dependent manner. These results of immunohistochem-

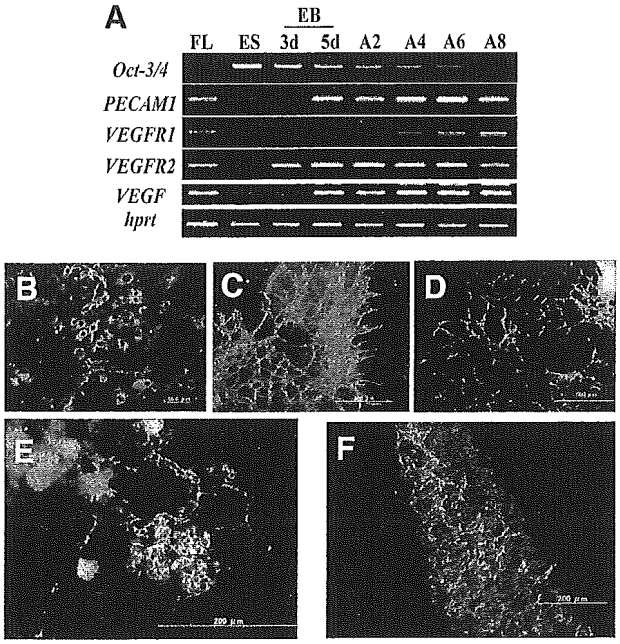

Figure 4. Hepatic morphogenesis derived from outgrowths of EBs consisting of albumin-positive hepatocytes and CD31/PECAM-1–positive endothelial cells expanding into vessel-network structures. **(A):** Endothelial development-associated gene expression was detected by reverse transcription–polymerase chain reaction analysis and activated during the differentiation of EBs. **(B):** Immunohistochemical analysis, with anti-albumin (red) and anti-CD31/PECAM-1 (green) antibodies, in mixed cultures of embryonic liver cells in vitro as a control. **(C, D):** CD31/PECAM-1–positive cells were shown to form a network structure in the presence of growth factors **(D)** and in the absence of growth factors **(C)**. The outgrowths of EBs at A18 were stained with CD31/PECAM-1 antibodies. Without exogenous growth factors, a part of the outgrowth EBs was shown as vessel-like formation. **(E, F):** Immunohistochemical analysis of the EB outgrowth at A10 **(E)** and A18 **(F)** using anti-albumin (red) and anti-CD31/PECAM-1 (green) antibodies in the absence of any growth factors. Abbreviations: EB, embryoid body; ES, embryonic stem; FL, mouse fetal liver at E15; PECAM-1, platelet-endothelial cell adhesion molecule-1; VEGFR, vascular endothelial growth factor receptor.

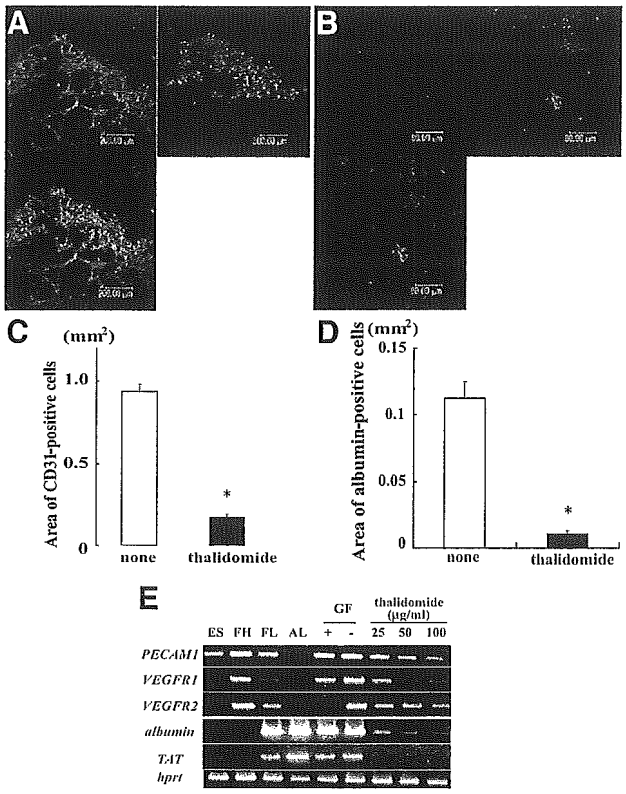

Figure 5. Dependence of hepatic morphogenesis depends on angiogenesis or vasculogenesis in the differentiated EBs. **(A, B):** Immunohistochemical analysis of the EB outgrowths at A18 using anti-CD31/PECAM-1 antibody in the presence of 100 μg/ml thalidomide for 18 days **(B)** and without thalidomide as a control **(A)**. **(C, D):** Quantitative analysis of the CD31/PECAM-1–positive area in the EB outgrowths at A18 was performed using the Scion image Beta 4.0.2 software in each of 15 selected individual fields from three independent experiments. Data are given as mean values ± standard error. Student's *t*-test for unpaired data was applied as appropriate. Difference of $p < .001$ was considered significant. **(E):** Endothelial cell and hepatocyte-associated gene expression was analyzed by reverse transcription–PCR in the thalidomide-treated EB outgrowths of the EBs at A18. PCR amplification of *PECAM-1*, *VEGFR1*, *VEGFR2*, and *TAT* was carried out for 40 cycles. Amplification of *albumin* was carried out for 30 cycles. Abbreviations: AL, mouse adult liver; ES, undifferentiated ES cells; FH, mouse fetal heart at E15; FL, mouse fetal liver at E15; GF, growth factor; PCR, polymerase chain reaction; PECAM-1, platelet-endothelial cell adhesion molecule-1; TAT, tyrosine aminotransferase; VEGFR, vascular endothelial growth factor receptor.

ical and RT-PCR analyses suggested that differentiation to endothelial cells was strongly inhibited by thalidomide. Expression of *albumin* and *TAT* was detected in the EBs at A18 in the absence, but not in the presence, of thalidomide (Fig. 5F).

Furthermore, to address the potential role of endothelial cell differentiation and proliferation in the growth of hepatocytes from ES cells, CBO-P11, a VEGF receptor–specific inhibitor, was added in this system. CD31/PECAM-1–positive cells were reduced by addition of CBO-P11 in the EB outgrowths at A18 compared with the control (Figs. 6A–6C). In the presence of CBO-P11, the morphology of the small CD31/PECAM-1–positive area was truncated and disconnected (Fig. 6B). Corresponding to the CD31/PECAM-1–positive cell populations, no albumin-positive cells were observed in the CBO-P11–treated EB outgrowths, whereas there were many albumin-positive cells in the control (Figs. 6A, 6B, 6D). The expression of *PECAM-1* was significantly lower in the CBO-P11–treated EB outgrowths than in the control without CBO-P11. Interestingly, no expression of albumin or TAT was detected in the EBs at A18 in the presence of CBO-P11 (Fig. 6F). The results of these experiments involving treatment with thalidomide and CBO-P11 suggest that CD31/PECAM-1–positive cells have a crucial role in the hepatic differentiation of ES cells.

Discussion

The purpose of this study was to devise an in vitro system that would allow liver morphogenesis from ES cells, reproducing the events of liver development in vivo. We first considered it necessary to promote the differentiation of outgrowths from EBs, derived from dissociated ES cells, to cardiomyocytes at high efficiency. Selected sublines from the parental ES cells showed a high frequency of emergence of cardiomyocytes and albumin-positive cells, whereas the frequency of cardiomyocyte emergence from the parental ES cells was not so high because of the heterogeneity of the ES cell culture in which albumin-positive cells failed to appear. The same effect was observed in our culture system, suggesting that the initial pluripotency of ES cells contributed to the differentiation of EBs to beating cardiomyocytes, and after induction to mesodermal lineages hepatic differentiation and maturation occurred in the EB outgrowths. Naggy et al. [23] described that recloned ES cell sublines could contribute significantly to the production of chimeric mice and for germ-line transmission in these mice compared with the parental line and could also become a complete body using ES cell–tetraploid aggregation [23, 24], because after a high number of passages, an ES cell culture is a heterogeneous mixture of undifferentiated and differentiated populations. It is very important for undifferentiated and pluripotent ES cells to be present in these cultures for differentiation not only to cardiomyocytes but also to albumin-producing hepatocytes and endothelial cells, corresponding to the various developmental stages of the liver. We tested several sublines of ES cells for their efficiency in the production of chimeric mice that would have the potential for germ-line transmission and a high frequency of cardiomyocyte emergence. It is interesting that the ES cell sublines that transmitted the germ line in chimeric mice at high efficiency corresponded to those with a frequency of cardiomyocyte emergence of almost 100%. The potential of ES cells to transmit the germ line in chimeric mice corresponded to the frequency of cardiomyocyte emergence in the EB outgrowths. We showed that albumin expression data in both emergence and non-

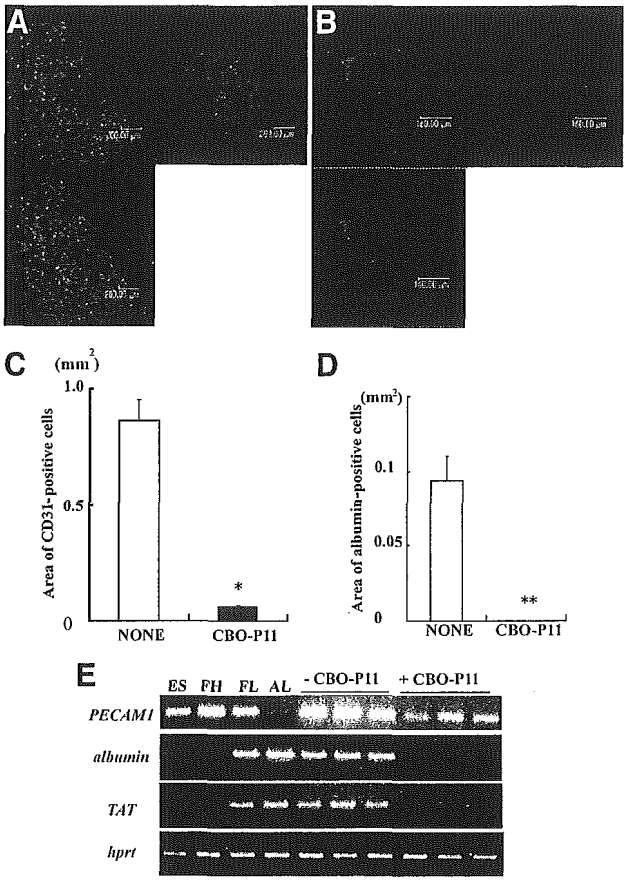

Figure 6. Lack of induction of hepatic morphogenesis by vascular endothelial growth factor inhibitor in the differentiated EBs. **(A, B):** Immunohistochemical analysis of the EB outgrowths at A18 using anti-CD31/PECAM-1 antibody in the presence of 10 μM CBO-P11 for 18 days **(B)** and without CBO-P11 as a control **(A)**. **(C, D):** Quantitative analysis of the CD31/PECAM-1–positive area in the EB outgrowths at A18 was performed using the same method as that for the thalidomide experiments in each of nine individual fields selected from three independent experiments. **(E):** Endothelial cell and hepatocyte-associated gene expression was analyzed by RT-PCR in the thalidomide-treated EB outgrowths at A18. PCR amplification of *PECAM-1* and *TAT* was carried out for 40 cycles. Amplification of albumin was carried out for 30 cycles. Abbreviations: AL, mouse adult liver; EB, embryoid body; ES, undifferentiated embryonic stem cells; FH, mouse fetal heart at E15; FL, mouse fetal liver at E15; PECAM-1, platelet-endothelial cell adhesion molecule-1; RT-PCR, reverse transcription–polymerase chain reaction; TAT, tyrosine aminotransferase.

emergence of cardiomyocytes, as shown in Figure 1B, although cardiomyocyte ablation and blocking cardiomyocyte differentiation experiments are very interesting. However, we consider that subclone screening for the frequency of emergence of cardiomyocytes from the parental murine ES cells would be useful for establishing an in vitro model of hepatic morphogenesis.

The number of albumin-producing cells increased cumulatively in the expanding vascular network area during differentiation to the late stage. It has been clarified that in vitro differentiation of murine ES cells within EBs leads to complex structures that can mimic the normal developmental process of the early embryo, in particular vasculogenesis and hematopoiesis, although no details of liver morphogenesis have been reported [25–27]. Our present results indicated that expansion of the endothelial cell network derived from ES cells plays an important role in the proliferation of hepatocytes and also liver morphogenesis in vitro, reproducing the events that occur in vivo. Furthermore, our liver morphogenesis system does not involve simple coculture of ES cells with endothelial cells prepared from liver sinusoids or blood vessels but is a novel system that utilizes the differentiation of pluripotent ES cells to cardiomyocytes to support subsequent differentiation to endothelial cells and hepatocytes. The interaction between hepatocytes and endothelial cells in liver organogenesis has already been reported by Matsumoto et al. [10]. Our in vitro system for the induction of liver morphogenesis from ES cells closely corresponds to the natural events of liver development that occur in vivo, as shown in Figure 7. Thalidomide, an inhibitor of angiogenesis, inhibited the differentiation and proliferation of CD31/PECAM-1–positive cells in EB outgrowths. However, there is a possibility that thalidomide may have directly suppressed the differentiation of hepatocytes. Therefore, to confirm the crucial role of endothelial cells in hepatic differentiation and maturation, we examined the effect of CBO-P11, a potent VEGF signal-specific inhibitor [28–30], in our culture system. CBO-P11 strongly suppressed the differentiation and proliferation of CD31/PECAM-1–positive cells, corresponding to endothelial cells, during EB differentiation, and consequently, the differentiation of albumin-positive cells, corresponding to hepatocytes, was completely blocked. These results were consistent with the data obtained from the thalidomide experiment.

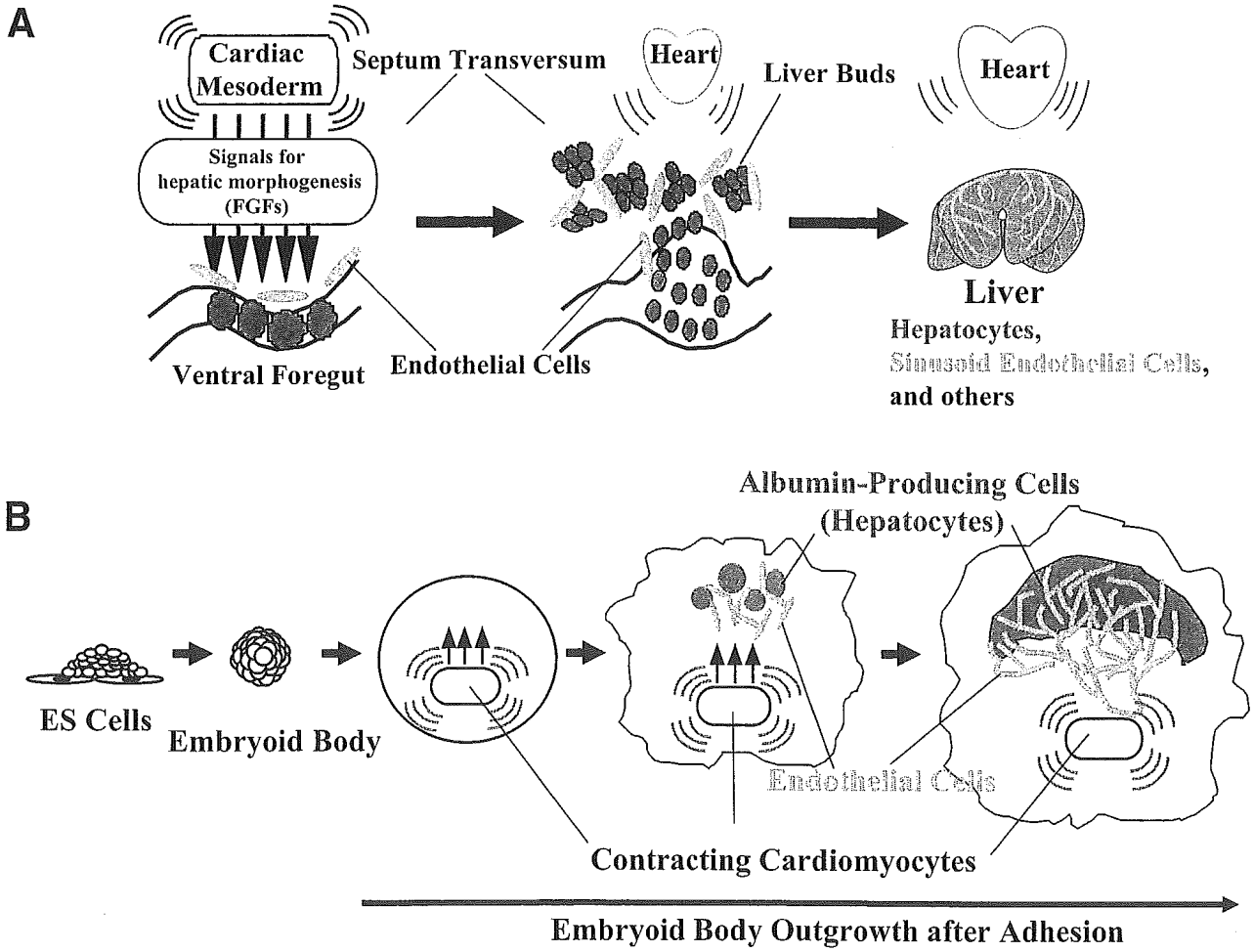

Figure 7. Illustrations of **(A)** in vivo liver development and **(B)** our in vitro system for the construction of hepatic organogenesis using murine ES cells. Abbreviations: ES, embryonic stem; FGF, fibroblast growth factor.

The process of organogenesis relies on the presence of specific microenvironments. However, it is difficult to reconstruct such microenvironments in vitro simply by addition of excess free molecules, such as FGF, HGF, and oncostatin M. Strategies for adding growth factors known as liver development inducers to the differentiation medium or for introducing an expression vector of a liver-specific master gene into ES cells can induce the expression of several specific genes in the area of cell interaction, which means that it is difficult to induce the differentiation of ES cell cultures to more than two cell lineages, such as hepatocytes and sinusoidal endothelial cells, through addition of these factors. These kinds of strategies make it impossible, or at least very difficult, to reconstruct target morphogenesis or to induce natural target cells with specific multiple functions. Therefore, no additional growth factors were used in our experiments. We succeeded in reconstructing in vitro the process of liver morphogenesis that involved at least three different types of cell populations: cardiomyocytes, endothelial cells, and hepatocytes. Initiation of liver organogenesis in vivo occurs in the septum transversum. The septum transversum mesenchyme also has important roles in liver organogenesis, such as production of HGF [9, 31]. In our present study, strong expression of HGF was detected in the ES differentiation system, as shown in Figure 2F. Although we detected many fibroblastic cells in this system, it was unclear whether some of these cells corresponded to the septum transversum. With regard to liver function, we were able to demonstrate ammonia degradation activity in this liver differentiation system (Fig. 2G). Unlike a primary hepatocyte culture, which contains almost 100% hepatocytes, our system contains a heterologous population including hepatocytes, endothelial cells, cardiomyocytes, and so on. However, the level of hepatic function, such as ammonia degradation, in each individual hepatocyte was higher in our differentiation system than in a primary culture, suggesting that hepatocyte–endothelial cell contact is very important for the generation of full hepatic function in hepatocytes, as well as for liver development and proliferation in the embryo. Generally, a hepatocyte primary culture has a short life span, shows no proliferation, and has low hepatic function. Therefore, we consider that a hepatocyte primary culture as a single-cell source is not sufficient for creation of a bioartificial liver system and that nonparenchymal cell populations are also necessary for reproducing the complex structure and polarity of the liver seen in vivo.

Here, we established a novel system for liver organogenesis from murine ES cells based on embryological events, i.e., with contributions from cardiac mesoderm and endothelial cell lineages, which were also derived from the ES cells. Furthermore, it has been difficult up to now to culture hepatocytes prepared from adult or embryonic liver in vitro for a long period, as well as to maintain the multiple functions characteristic of the liver. This is one of the major obstacles to the development of a bioartificial liver system. Our system makes it possible to culture ES cell–derived hepatocytes for a long period, at least for more than 30 days, and these cells are able maintain a high degree of hepatic function (Fig. 2F). This innovative system will be useful for creation of liver embryology and regeneration systems as well as for the development of a bioartificial liver system for bridging use in patients waiting for a liver donor and for drug-metabolism assays.

Acknowledgments

We are grateful to Prof. Nobuaki Yoshida and Prof. Yoichiro Iwakura (Institute of Medical Science, University of Tokyo, Toyko) for providing E14.1 ES cells, Prof. Hisato Kondo (Institute for Molecular and Cellular Biology, Osaka University, Osaka, Japan) for NHL7 cells, RIKEN Cell Bank for STO and HePa 1-6 cell lines, and General Research Laboratory, Shinshu University School of Medicine, Nagano, Japan, for technical assistance. This study was supported by grants from the Ministry of Education, Sports, Science and Technology of Japan (Tokyo) (15700314; 13470150, Grant-in-Aid for 21st Century COE program by the above ministry), Hokuto Foundation of Bioscience (Nagano, Japan), and Foundation of Shinshu Igakushinko (Matsumoto, Japan).

References

1 Zaret KS. Regulatory phases of early liver development: paradigms of organogenesis. Nat Rev Genet 2002;3:499–512.

2 Reif S, Terranova VP, el-Bendary M et al. Modulation of extracellular matrix proteins in rat liver during development. Hepatology 1990;12:519–525.

3 Kamiya A, Kojima N, Kinoshita T et al. Maturation of fetal hepatocytes in vitro by extracellular matrices and oncostatin M: induction of tryptophan oxygenase. Hepatology 2002;35:1351–1359.

4 Gualdi R, Bossard P, Zheng M et al. Hepatic specification of the gut endoderm in vitro: cell signaling and transcriptional control. Genes Dev 1996;10:1670–1682.

5 Couvelard A, Bringuier AF, Dauge MC et al. Expression of integrins during liver organogenesis in humans. Hepatology 1998;27:839–847.

6 Jung J, Zheng M, Goldfarb M et al. Initiation of mammalian liver development from endoderm by fibroblast growth factors. Science 1999;284:1998–2003.

7 Fukuda-Taira S. Hepatic induction in the avian embryo: specificity of reactive endoderm and inductive mesoderm. J Embryol Exp Morphol 1981;63:111–125.

8 Douarin NM. An experimental analysis of liver development. Med Biol 1975;53:427–455.

9 Rossi JM, Dunn NR, Hogan BL et al. Distinct mesodermal signals, including BMPs from the septum transversum mesenchyme, are required in combination for hepatogenesis from the endoderm. Genes Dev 2001;15:1998–2009.

10 Matsumoto K, Yoshitomi H, Rossant J et al. Liver organogenesis promoted by endothelial cells prior to vascular function. Science 2001;294:559–563.

11 Sherer GK. Tissue interaction in chick liver development: a reevaluation, I. Epithelial morphogenesis: the role of vascularity in mesenchymal specificity. Dev Biol 1975;46:281–295.

12 Bankston PW, Pino RM. The development of the sinusoids of fetal rat liver: morphology of endothelial cells, Kupffer cells, and the transmural migration of blood cells into the sinusoids. Am J Anat 1980;159:1–15.

13 Enzan H, Himeno H, Hiroi M et al. Development of hepatic sinusoidal structure with special reference to the Ito cells. Microsc Res Tech 1997;39:336–349.

14 Hamazaki T, Iiboshi Y, Oka M et al. Hepatic maturation in differentiating embryonic stem cells in vitro. FEBS Lett 2001;497:15–19.

15 Yamamoto H, Quinn G, Asari A et al. Differentiation of embryonic stem cells into hepatocytes: biological functions and therapeutic application. Hepatology 2003;37:983–993.

16 Yamada T, Yoshikawa M, Kanda S et al. In vitro differentiation of embryonic stem cells into hepatocyte-like cells identified by cellular uptake of indocyanine green. STEM CELLS 2002;20:146–154.

17 Yin Y, Lim YK, Salto-Tellez M et al. AFP(+), ESC-derived cells engraft and differentiate into hepatocytes in vivo. STEM CELLS 2002;20:338–346.

18 Jones EA, Tosh D, Wilson DI et al. Hepatic differentiation of murine embryonic stem cells. Exp Cell Res 2002;272:15–22.

19 Chinzei R, Tanaka Y, Shimizu-Saito K et al. Embryoid-body cells derived from a mouse embryonic stem cell line show differentiation into functional hepatocytes. Hepatology 2002;36:22–29.

20 Lavon N, Yanuka O, Benvenisty N. Differentiation and isolation of hepatic-like cells from human embryonic stem cells. Differentiation 2004;72:230–238.

21 Horai R, Asano M, Sudo K et al. Production of mice deficient in genes for interleukin (IL)-1α, IL-1β, IL-1α/β, and IL-1 receptor antagonist shows that IL-1β is crucial in turpentine-induced fever development and glucocorticoid secretion. J Exp Med 1998;187:1463–1475.

22 Itoh H, Abo T, Sugawara S et al. Age-related variation in the proportion and activity of murine liver natural killer cells and their cytotoxicity against regenerating hepatocytes. J Immunol 1988;141:315–323.

23 Nagy A, Rossant J, Nagy R et al. Derivation of completely cell culture-derived mice from early-passage embryonic stem cells. Proc Natl Acad Sci U S A 1993;90:8424–8428.

24 Auerbach W, Dunmore JH, Fairchild-Huntress V et al. Establishment and chimera analysis of 129/SvEv- and C57BL/6-derived mouse embryonic stem cell lines. Biotechniques 2000;29:1024–1028, 1030, 1032.

25 Wartenberg M, Gunther J, Hescheler J et al. The embryoid body as a novel in vitro assay system for antiangiogenic agents. Lab Invest 1998;78:1301–1314.

26 Hirashima M, Kataoka H, Nishikawa S et al. Maturation of embryonic stem cells into endothelial cells in an in vitro model of vasculogenesis. Blood 1999;93:1253–1263.

27 Wang R, Clark R, Bautch VL. Embryonic stem cell-derived cystic embryoid bodies form vascular channels: an in vitro model of blood vessel development. Development 1992;114:303–316.

28 Bikfalvi A. Recent developments in the inhibition of angiogenesis: examples from studies on platelet factor-4 and the VEGF/VEGFR system. Biochem Pharmacol 2004;68:1017–1021.

29 Bello L, Lucini V, Costa F et al. Combinatorial administration of molecules that simultaneously inhibit angiogenesis and invasion leads to increased therapeutic efficacy in mouse models of malignant glioma. Clin Cancer Res 2004;10:4527–4537.

30 Zilberberg L, Shinkaruk S, Lequin O et al. Structure and inhibitory effects on angiogenesis and tumor development of a new vascular endothelial growth inhibitor. J Biol Chem 2003;278:35564–35573.

31 Andermarcher E, Surani MA, Gherardi E. Co-expression of the HGF/SF and c-met genes during early mouse embryogenesis precedes reciprocal expression in adjacent tissues during organogenesis. Dev Genet 1996;18:254–266.

Transplant International ISSN 0934-0874

ORIGINAL ARTICLE

MCI-186 (edaravone), a free radical scavenger, attenuates hepatic warm ischemia–reperfusion injury in rats

Fumitaka Suzuki,[1,2] Yasuhiko Hashikura,[2] Hirohiko Ise,[1] Akiko Ishida,[3] Jun Nakayama,[3] Masafumi Takahashi,[1] Shin-ichi Miyagawa[2] and Uichi Ikeda[1]

1 Department of Organ Regeneration, Shinshu University Graduate School of Medicine, Asahi, Matsumoto, Japan
2 First Department of Surgery, Shinshu University School of Medicine, Asahi, Matsumoto, Japan
3 Department of Pathology, Shinshu University School of Medicine, Asahi, Matsumoto, Japan

Keywords
chemokine, Kupffer cell, lipid peroxidation, macrophage, neutrophil.

Correspondence
Yasuhiko Hashikura MD, First Department of Surgery, Shinshu University School of Medicine, 3-1-1 Asahi, Matsumoto 390-8621, Japan. Tel.: +81-263-37-2654; fax: +81-263-35-1282; e-mail: yh@hsp.md.shinshu-u.ac.jp

Received: 17 November 2004
Revision requested: 7 December 2004
Accepted: 20 December 2004

doi:10.1111/j.1432-2277.2005.00094.x

Summary

Hepatic warm ischemia–reperfusion injury (IRI) during hepatectomy and liver transplantation is a major cause of liver dysfunction in which the pathologic role of free radicals is a major concern. To assess the effect of MCI-186 (edaravone) on hepatic IRI, male Wistar rats were subjected to partial hepatic ischemia for 60 min after pretreatment with vehicle (group C) or MCI-186 (group M), or after both MCI-186 pretreatment and additional administration of MCI-186 12 h after reperfusion (group MX). Groups M and MX showed significantly lower levels of serum alanine aminotransferase and hepatic lipid peroxidation than group C, and also significantly lower expression levels of mRNA for cytokines, chemokines and intercellular adhesion molecule-1. There were fewer tissue monocytes and neutrophils in groups M and MX than in group C. These effects were more marked in group MX than in group M. Our findings suggest that treatment with MCI-186 attenuates hepatic IRI in this rat *in vivo* model.

Introduction

Warm ischemia–reperfusion injury (IRI) during hepatic resection and liver transplantation may lead to local and systemic organ dysfunction. The local hepatic injury comprises two phases, the acute (early) phase and the subacute (late) phase [1–9]. During the acute phase, Kupffer cells are activated and release oxygen-derived free radicals (ODFRs) and proinflammatory cytokines such as tumor necrosis factor (TNF)-α, interleukin (IL)-1, IL-6 and IL-8. The subacute phase is mediated by infiltrating neutrophils that are primed and activated during the acute phase [1–9]. Chemokines released by Kupffer cells, including CXC chemokines and CC chemokines, may also play important roles in hepatic IRI. CXC chemokines induce neutrophil activation and CC chemokines activate macrophages and T cells and upregulate cell adhesion molecules [10–13]. While recent studies have shown that not only macrophages (Kupffer cells) and neutrophils but also T cells play significant roles in hepatic IRI [3,5,6,14,15], the significance of free radicals in the pathology of the acute and subacute phases of hepatic IRI is thought to be crucial.

MCI-186 [edaravone (3-methyl-1-phenyl-2-pyrazolin-5-one); Mitsubishi Pharma Co., Osaka, Japan] is a free radical scavenger. This reagent has already been applied clinically for the prevention of brain edema in patients with acute cerebral infarction through inhibition of the lipoxygenase pathway in the arachidonic acid cascade and has shown positive results [16–19]. Several reports have described the effects of MCI-186 on hepatic IRI. In *ex vivo* hepatic IRI experiments [20,21], perfusion with Krebs–Henseleit solution cannot reproduce the effects of circulating macrophages and neutrophils, which play major roles in hepatic IRI. In *in vivo* experiments, the efficacy of MCI-186 in attenuating hepatic warm IRI has been evaluated in terms of aspartate aminotransferase, phosphatidylcholine hydroperoxide, adenosine triphosphate [22], and mitochondrial function [23]. However,

the effects of MCI-186 on monocytes, neutrophils and their associated cytokines have not been evaluated.

In the present study, we evaluated the potential of MCI-186 to attenuate hepatic warm IRI in a partial-IRI rat model *in vivo*. We focused on the changes in lipoxygenase activation, monocyte activation, chemokine expression, neutrophil infiltration and hepatic dysfunction resulting from administration of MCI-186.

Materials and methods

Experimental animals and reagents

Male Wistar rats (Clea Japan Inc., Tokyo, Japan) weighing 200–250 g were used. All animals were maintained under standard conditions and fed rodent chow and water *ad libitum*. Twelve hours before surgery, the animals were fasted, but allowed access to water. All experimental procedures were reviewed and approved by the Institutional Animal Care and Use Committee of Shinshu University.

The following monoclonal antibodies were used as primary antibodies for immunohistochemistry: HNEJ-2 (Nikken Seil Co., Shizuoka, Japan) specific for 4-hydroxy-2-nonenal (4-HNE) modified protein, ED-1 (Serotec, Oxford, UK) specific for rat CD163 expressed on free and fixed macrophages, ED-2 (Serotec) specific for rat CD68 expressed on Kupffer cells and on residential macrophages, and HIS48 (BD Biosciences, Palo Alto, CA, USA) specific for rat neutrophils.

Hepatic IRI model

All surgical procedures were carried out according to the protocol described elsewhere [24]. Rats were anesthetized with sodium pentobarbital 50 mg/kg, intraperitoneally (Dainippon Pharmaceutical Co. Ltd, Osaka, Japan). After laparotomy, a microvascular clip (BEAR Medic Co., Chiba, Japan) was used to interrupt the arterial and portal venous supply to the median and left lateral lobes of the liver. This resulted in ischemia of approximately 70% of the whole liver while avoiding portal venous congestion. After 60 min of partial hepatic ischemia, the clamp was removed for reperfusion. The abdomen was closed and 1 ml of saline was administered intravenously. The rats were killed 1, 3, 6 and 24 h after reperfusion, and blood and tissue samples were harvested for analysis.

Experimental protocol

The rats were divided into three groups(Fig. 1). Group S was a sham operation group. Group C comprised IRI model rats, administered saline 5 min before reperfusion. Group M comprised IRI model rats, administered MCI-186 (3 mg/kg) 5 min before reperfusion. Saline and MCI-186 were injected intravenously. The dose and timing of saline and MCI-186 administration were based on previous reports [25–27].

Each group was divided into four subgroups according to the time (h) from reperfusion to killing [groups S-1, S-3, S-6, S-24 ($n = 5$, respectively), C-1 ($n = 6$), C-3 ($n = 5$), C-6 ($n = 7$), C-24 ($n = 7$), M-1 ($n = 6$), M-3 ($n = 5$), M-6 ($n = 7$) and M-24 ($n = 5$)]. For groups S-24, C-24 and M-24, additional administration of saline was performed 12 h after reperfusion.

In addition, considering the short half-life of MCI-186 as well as the acute and subacute mechanisms underlying IRI, a fourth group was additionally administered MCI-186 12 h after reperfusion instead of saline, followed by killing 24 h after reperfusion [group MX-24 ($n = 7$)]. This protocol was used to evaluate the role of MCI-186 in the subacute phase of IRI.

Peripheral blood and tissue samples

Blood samples were obtained via the abdominal aorta. The blood was centrifuged (2500 *g*, 10 min) at room temperature and the plasma was collected and stored at −20 °C until use. Portions of the ischemic and nonischemic lobes were fixed in 10% buffered formalin and embedded in paraffin. Other portions were snap-frozen in

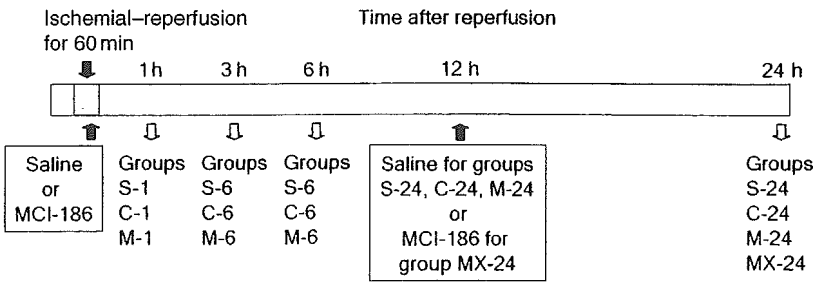

Figure 1 Experimental protocols for rat hepatic ischemia–reperfusion injury models.

liquid nitrogen to extract mRNA and embedded in optimal cutting temperature (OCT) compound (Sakura Finetechnical Co., Tokyo, Japan) for immunohistochemistry, and stored at −80 °C until used.

Measurement of serum aminotransferase

To evaluate hepatic injury, we measured serum alanine aminotransferase (ALT) levels at the time of killing in each group using an AU5232 autoanalyzer (Olympus, Tokyo, Japan), as described previously [24].

Histologic examination

Samples were fixed with 10% buffered formaldehyde and embedded in paraffin. Sections at 3-μm intervals were prepared and stained with hematoxylin and eosin for histologic examination. A blinded analysis was performed by two pathologists to determine the degree of lesions observed ($n = 5$, independent animals in each group). The degrees of sinusoidal congestion, cytoplasmic vacuolization and necrosis of parenchymal cells were evaluated semiquantitatively according to the criteria described in a previous study [28].

Immunohistochemistry

Immunohistochemical detection of lipid peroxidation and inflammatory cell recruitment was carried out. For detection of 4-HNE and macrophages, 10% buffered formaldehyde-fixed and paraffin-embedded tissue samples were cut into 3-μm-thick sections. Antigen retrieval was performed by 25 min of microwave irradiation in 1.0 mM EDTA-Na_2 for 4-HNE, and by 6 min of proteinase K digestion (0.4 mg/ml) for ED-2. No retrieval procedure was performed for ED-1. After antigen retrieval, the sections were incubated with primary antibodies at 4 °C overnight for 4-HNE and at room temperature for 60 min for ED-1 and ED-2. The dilutions of the primary antibodies were 1:80 for 4-HNE, 1:200 for ED-1 and 1:100 for ED-2. Goat anti-mouse immunoglobulin conjugated with peroxidase-labeled dextran polymer (Envision™+ system; Dako, Carpinteria, CA, USA) was used as the secondary antibody.

For detection of neutrophils, we used frozen sections. Samples embedded in OCT compound were cut into 5-μm-thick sections, placed on adhesive-coated slides (Matsunami Glass, Osaka, Japan), and then air-dried. After blocking with 1% normal goat serum in tris-buffered saline, these tissue specimens were incubated at room temperature for 60 min with a primary monoclonal antibody, HIS48. After washing with phosphate-buffered saline, the specimens were incubated using the Envision™+ system.

In a control experiment, the primary antibody was omitted from the staining procedure, and no specific staining was found. Counterstaining was carried out with hematoxylin.

Analysis of mRNA by reverse transcription-polymerase chain reaction (RT-PCR)

Total RNA was extracted from tissue with ISOGEN (Nippon Gene Co. Ltd, Tokyo, Japan). cDNA was reverse-transcribed from 2 μg of total RNA using an Omniscript™ Reverse Transcriptase kit (Qiagen GmbH, Hilden, Germany). The cDNA was amplified by RT-PCR using a *Taq* polymerase core kit (Qiagen GmbH). We prepared primer sets for RT-PCR as shown in Table 1, and the final reaction volume was 25 μl. The samples were loaded into a thermal cycler after determining the optimal number of cycles as follows: 30 cycles of denaturing at 94 °C for 1 min, annealing at 55 °C for 1 min, and extension at 72 °C for 2 min for TNF-α and IL-1β; 30 cycles at 94 °C for 30 s, 58 °C for 1 min, and 72 °C for 1 min for cytokine-induced neutrophil chemoattractant (CINC)-2 and macrophage inflammatory protein (MIP)-2; 25 cycles at 94 °C for 30 s, 60 °C for 1 min, and 72 °C

Table 1. Polymerase chain reaction primer sets for cytokines, chemokines, and adhesion molecule.

	Sense (5′ → 3′)	Anti-sense (5′ → 3′)
β-actin	CGG CAT TGT AAC CAA CAG G	CAT TGC CGA TAG TGA TGA CC
TNF-α	TAC TGA ACT TCG GGG TGA TTG GTC C	CAG CCT TGT CCC TTG AAG AGA A
IL-1β	GCT ACC TAT GTC TTG CCC GT	GAC CAT TGC TGT TTC CTA GG
CINC-2	GCT ACC TAT GTC TTG CCC GT	TGA CCA TCC TTG GAG AGT GGC
MIP-2	AGC TCC TCA ATG CTG TAC TGG	TCT ATC ACA GTG TGG AGG TGG
MCP-1	CTC TTC CTC CAC CAC TAT GC	CTC TGT CAT ACT GGT CAC TTC
MIP-1α	GAA GGA AAG TCT TCT CAG CG	AGA CAT TCA GTT CCA GC
MIP-1β	ATG AAG CTC TGC GTG TCT GC	AGT TCC GAT GAA TCT TCC GG
ICAM-1	GAT GCT GAC CCT CCA CAC CA	CAG GGA CTT CCC ATC CAC CT

TNF-α, tumor necrosis factor alpha; IL-1β, interleukin-1 beta; CINC-2, cytokine-induced neutrophil chemoattractant-2; MIP, macrophage inflammatory protein; MCP, monocyte chemoattractant protein; ICAM-1, intercellular adhesion molecule-1.

for 1 min for monocyte chemoattractant protein (MCP)-1; 30 cycles at 94 °C for 30 s, 56 °C for 1 min, and 72 °C for 1 min for MIP-1α; 30 cycles at 94 °C for 30 s, 60 °C for 1 min, and 72 °C for 1 min for MIP-1β; and 30 cycles at 94 °C for 45 s, 55 °C for 30 s, and 72 °C for 90 s for intercellular adhesion molecule (ICAM)-1. The housekeeping gene β-actin was used as the RT-PCR control, and its cycling program was 25 cycles at 94 °C for 30 s, 60 °C for 1 min, and 72 °C for 1 min. For every gene, the final cycle was followed by soaking for 7 min at 72 °C. RT-PCR products were analyzed using 2.0% agarose gel electrophoresis, and visualized by staining with ethidium bromide.

Statistical analysis

Differences among the groups were evaluated by the Mann–Whitney *U*-test. All values are expressed as mean ± SEM, and data were considered significant at $P < 0.05$.

Results

Serum ALT levels at 1, 3, 6 and 24 h after reperfusion

The serum ALT levels in each group are shown in Fig. 2. Among the groups that underwent ischemia–reperfusion, ALT increased to 11207 ± 1957 U/l in group C-6, but decreased to 3782 ± 1334 U/l in group M-6, which was significantly lower than the level in group C-6. The effect of MCI-186 became less prominent 24 h after reperfusion.

Consequently, we focused on changes occurring 24 h after reperfusion. The ALT levels were 5445 ± 1155 U/l (group C-24) vs. 4405 ± 1387 U/l (group M-24). However, additional administration of MCI-186 at 12 h after reperfusion markedly inhibited the increase in ALT levels to 1065 ± 605 U/l (group MX-24).

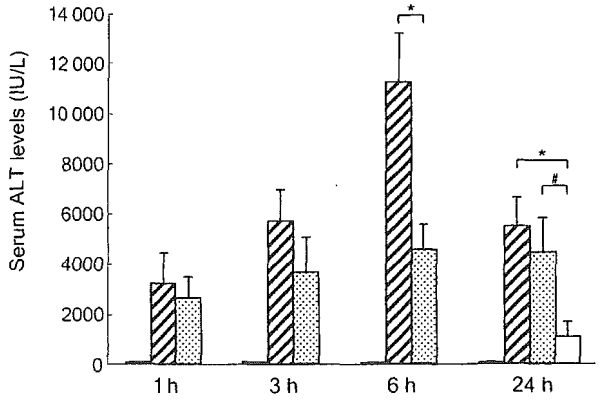

Figure 2 Effects of MCI-186 on serum alanine aminotransferase (ALT) levels. In the acute phase, rats treated with MCI-186 (group M) had lower ALT levels than the saline-treated group (group C). The ALT level in group MX-24 was significantly lower than that in groups C-24 and M-24. Values are expressed as mean ± SEM. *$P < 0.05$ compared with group C; #$P < 0.05$ compared with group M-24. ■, group S; ▨, group C; ▩, group M; □, group MX.

Histologic analysis

No pathologic findings were observed in the liver tissues of the sham control groups (data not shown). In group C-6, liver specimens exhibited focal necrosis, sinusoidal congestion and infiltration of leukocytes, and these changes became more severe in group C-24 (Fig. 3). In contrast, such findings were minimal in group M-6, but were observed in group M-24. In group MX-24, pathologic findings of spotty necrosis, sinusoidal congestion and infiltration of leukocytes were minimal compared with groups C-24 and M-24. These results were confirmed by a semi quantitative assessment, and shown to be significant (Table 2).

Immunohistochemistry for 4-HNE detection

There were no 4-HNE-positive cells in the liver in the sham control groups (data not shown). In groups C-6 and C-24, 4-HNE-positive cells were observed, but the 4-HNE levels were demonstrably reduced in group M-6 (Fig. 4). The number of 4-HNE-positive cells was lower in group MX-24 than in groups C-24 and M-24.

Immunohistochemistry for infiltrating cells

The numbers of cells positive for ED-1 (free macrophages) and ED-2 (resident macrophages) in the ischemic lobes were increased in group C-6, but not in group M-6 (Fig. 5a and b). However, such cells were increased to some extent in group M-24. In group MX-24, the numbers of both ED-1 and ED-2 positive cells were markedly reduced in comparison with groups C-24 and M-24. Figure 5c shows a similar tendency of infiltrated neutrophils into the sinusoids.

Expression of cytokine and chemokine mRNAs

Expression of cytokine and chemokine genes in the ischemic hepatic lobes in groups C and M was compared with that in group S, the sham control group (Fig. 6a). Expression of TNF-α mRNA was high after 1 h (group C-1) and then gradually decreased with time, and was lower in group M-1 than in group C-1 (Fig. 6b). Expression of IL-1 mRNA was high in groups C-1, C-3 and C-6, but attenuated in groups M-3 and M-6. The expression levels of CINC-2 (rat IL-8), MIP-2, MCP-1, MIP-1α and MIP-1β mRNAs were increased in groups C-3 and

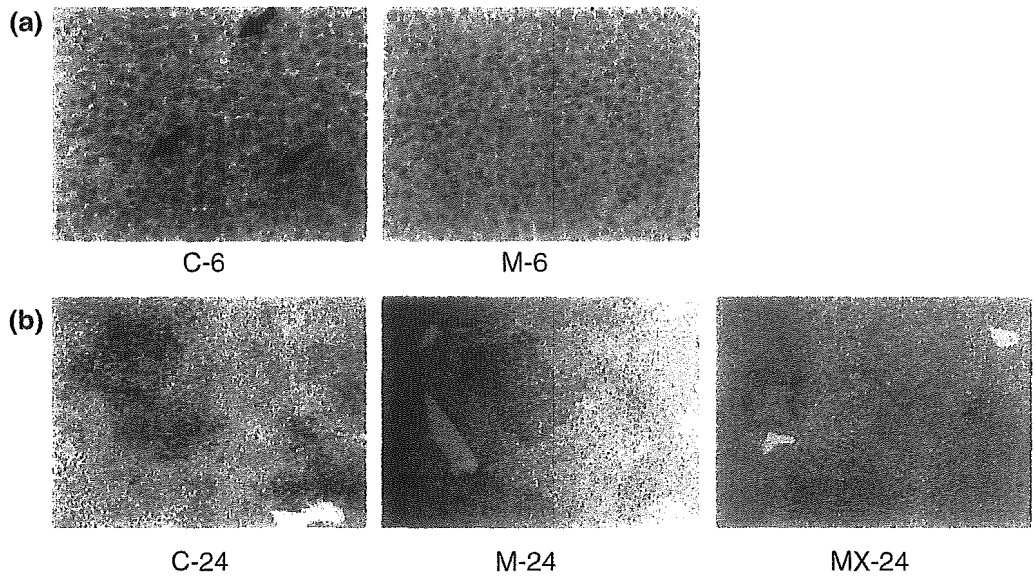

Figure 3 Representative histologic findings in the excised livers at 6 h and 24 h after reperfusion. (a) At 6 h after reperfusion, focal necrosis (arrows) and sinusoidal congestion were observed in the control group (group C-6) but not in the MCI-186-treated group (group M-6). Original magnification ×400. (b) At 24 h after reperfusion, spotty necrosis, ballooning of parenchymal cells, and more severe sinusoidal congestion were seen in the control group (group C-24) and also in the MCI-186-treated group (group M-24) but not in group MX-24 (original magnification ×100).

Table 2. Numerical degree of histologic damage according to the criteria advocated by Suzuki *et al.* (28). Congestion, vacuolization, and necrosis in liver tissue were estimated.

Groups	*Congestion*	*Vacuolization*	*Necrosis*
C-6	3.67 ± 0.21	0.67 ± 0.21	3.33 ± 0.21
M-6	2.33 ± 0.33*	0.50 ± 0.22	2.33 ± 0.21*
C-24	3.17 ± 0.17	3.50 ± 0.22	3.83 ± 0.17
M-24	2.83 ± 0.17	2.33 ± 0.21*	3.67 ± 0.21
MX-24	1.67 ± 0.21*,**	1.83 ± 0.31*	2.50 ± 0.22*,**

*$P < 0.05$ compared with group C.
**$P < 0.05$ compared with group M-24.

C-6, but those of the mRNAs for chemokines CINC-2, MIP-2, MCP-1 and MIP-1α were significantly decreased in group M-6. Expression of MIP-1β mRNA was not suppressed by MCI-186 at any time point. Figure 6c shows the expression of cytokine and chemokine mRNAs at 24 h. Expression was still high in group C-24, and CINC-2 and MIP-2 mRNA expression was suppressed significantly in group M-24. However, no suppression of IL-1, MCP-1, MIP-1α, and MIP-1β mRNA expression was evident. In group MX-24, the expression levels of mRNAs for all cytokines and chemokines were low. The differences in the expression levels of IL-1, MCP-1, MIP-1α and MIP-1β mRNAs were significant in comparison with groups C-24 and M-24.

We also investigated ICAM-1 mRNA expression at 6 h, as shown in Fig. 7. ICAM-1 mRNA expression was high 6 h after reperfusion (group C-6) and gradually decreased thereafter. The expression was significantly reduced in group M-6.

Discussion

We have investigated the usefulness of MCI-186 for the prevention of hepatic warm IRI in a rat model. The results demonstrate that administration of MCI-186 before reperfusion suppressed IRI in the acute phase, but did not result in sufficient suppression in the subacute phase. Additional administration of MCI-186 12 h after reperfusion also suppressed IRI in the subacute phase. This additional administration is presumably necessary because of the short half-life of MCI-186 and the multistep nature of hepatic IRI [1–9].

Free radicals are one of the important factors responsible for hepatic IRI [2–5,29], and several investigators have reported that free radical scavengers attenuate hepatic IRI [3–5,30–35]. Nevertheless, no such scavenger has been used clinically to date recently. MCI-186 is now used clinically and is beneficial after cerebral infarction. There have been several reports describing beneficial effect of MCI-186 on hepatic IRI, e.g. it attenuates liver injury at acute phase [22], it protects against mitochondrial injury [23] and it ameliorates cold IRI [20] or warm IRI [21] in isolated liver perfusion model using Krebs–Henseleit solution. However, none of these studies have focused on the effects of this reagent against various chemical

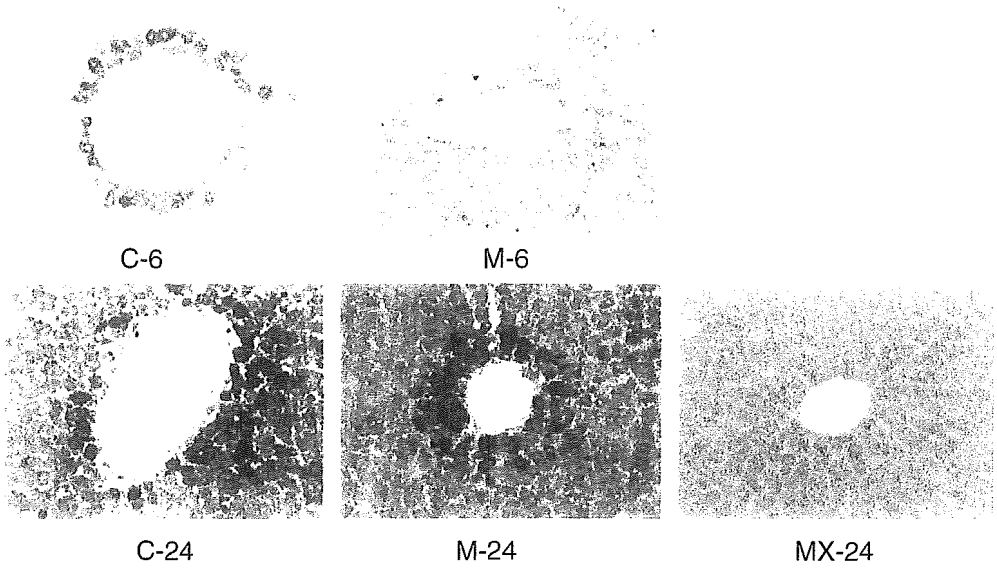

Figure 4 Representative findings of lipid peroxidation immunostaining with monoclonal antibody against 4-hydroxy-2-nonenal (4-HNE) modified proteins in rat livers at 6 h and 24 h after reperfusion. In groups C-6 and C-24, 4-HNE-positive cells were observed. Although 4-HNE staining was faint in group M-6, the number of 4-HNE-positive cells in group M-24 was comparable with that in group C-24. The number of 4-HNE-positive cells was decreased in group MX-24, compared with groups C-24 and M-24 (original magnification ×400).

mediators such as free radicals, cytokines and chemokines, inflammatory cells, adhesion molecules, and also against histologic damage in hepatic IRI model *in vivo*.

The ODFRs activate monocytes (resident or free) and induce nuclear factor κB in hepatic IRI, causing hepatic injury in the early phase [8,12,31,36–38]. TNF-α and IL-1β are potent proinflammatory cytokines secreted mainly by Kupffer cells during hepatic IRI [2–6,8,39,40]. These cytokines induce IL-8 and CINC-2 synthesis [4,41] and upregulate the expression of adhesion molecules such as Mac-1 or ICAM-1 [3,4]. TNF-α also induces chemokines such as epithelial neutrophil-activating protein 78, which plays an important role in neutrophil chemotaxis and activation, and stimulates ODFR production by Kupffer cells [2,4,7,42,43]. IL-1β induces Kupffer cells to produce TNF-α, upregulates ODFR production by neutrophils [4], and also upregulates the expression of nuclear factor κB and CXC chemokines [8]. In this study, the expression of TNF-α and IL-1β was elevated in the early phase after reperfusion, and attenuated in the MCI-186-treated groups.

MCP-1, MIP-1α and MIP-1β are CC chemokines, which exert a chemotactic effect on monocytes and T cells [10–13]. The expression levels of MCP-1 and MIP-1α were reduced in the MCI-186-treated group 3 h and 6 h (acute phase) after reperfusion. MCI-186 reduced monocyte infiltration into the liver, and this might have resulted from suppressed expression of CC chemokines. In the early phase of hepatic IRI, ODFR-stimulated Kupffer cells release MCP-1 [12], upregulates ICAM-1 expression on endothelial cells *in vitro* [44]. Up-regulation of ICAM-1 is one of the important factors involved in the pathogenesis of neutrophil-induced hepatic IRI [45]. These correlations appear to be supported by the present *in vivo* data indicating that suppression of MCP-1 and ICAM-1 expression in the MCI-186-treated groups led to a decrease in monocyte and neutrophil infiltration.

Similar mRNA expression patterns were also observed for members of the CXC chemokine superfamily (CINC-2 and MIP-2). CXC chemokines have potent chemotactic effects on neutrophils. Kupffer cells produce CINC when stimulated with ODFR generated by hypoxanthine and xanthine oxidase [2,3,41], while CINC-2 production can be reduced with a calcium channel blocker [41]. The level of CINC-2 is increased for several hours after reperfusion in rat liver IRI models [2,41]. MIP-2 is also upregulated in early hepatic or renal IRI and has an important role in neutrophil recruitment and organ injury [7,9,13]. Our results indicate that CINC-2 and MIP-2 levels were elevated in the early phase of IRI in the control groups, and we suspect a correlation between the expression of CXC chemokines and neutrophil infiltration. This inference is supported by the observation that both CXC chemokine expression and neutrophil infiltration were suppressed in the MCI-186-treated groups.

In our study, single administration of MCI-186 did not have attenuated infiltration of neutrophils or macrophages in the subacute phase presumably because of its short

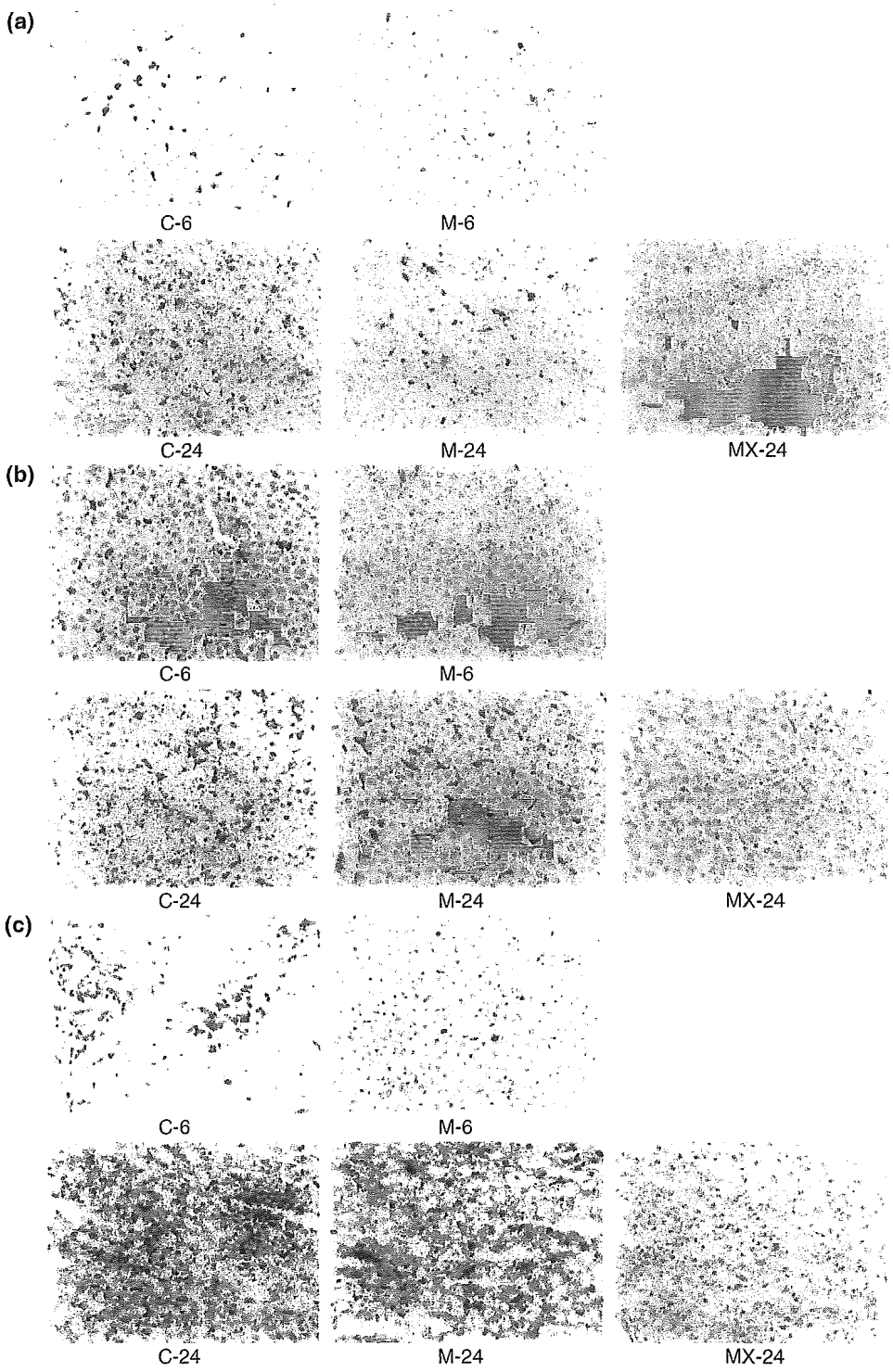

Figure 5 Immunohistochemistry for inflammatory cells in the liver tissues. (a) ED-1-positive cells (resident macrophages). (b) ED-2-positive cells (free macrophages). (c) Neutrophils. The numbers of ED-1- and ED-2-positive cells in the ischemic lobes were increased in group C-6 but absent in group M-6. In group M-24, the numbers of ED-1- and ED-2-positive cells in the ischemic lobes were increased. In group MX-24, the number of macrophages was markedly reduced. Infiltration of neutrophils into the sinusoids was observed in groups C-6 and C-24. Infiltration was suppressed in group M-6, but not in group M-24. In group MX-24, infiltration of neutrophils into sinusoids was demonstrably reduced (original magnification ×400).